EXPERIMENTAL INVESTIGATIONS INTO THE DYNAMIC RESPONSE OF A LATHE BED
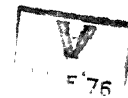
A Thesis Submitted

In Partial Fulfilment of the Requirements

for the Degree of
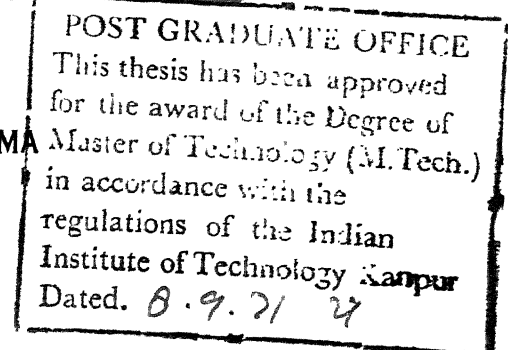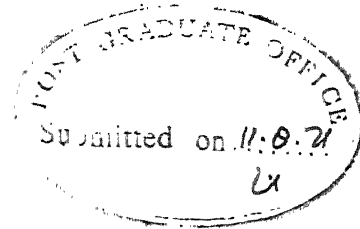
MASTER OF TECHNOLOGY

BY
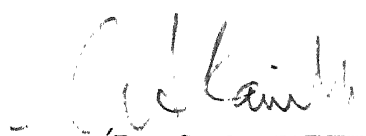
KRISHNA MURTI LOOBMA

to the

DEPARTMENT OF MECHANICAL ENGINEERING

INDIAN INSTITUTE OF TECHNOLOGY KANPUR

AUGUST 1971

CERTIFICATE

This is to certify that the thesis entitled
"Experimental Investigations into the dynamic response of
a lathe bed" has been carried out under my supervision and
that the results embodied in this thesis have not been sub-
mitted to anyother institute or university for award of any
degree.

(Dr. G. S. KAINTH)
Assistant Professor
Department of Mechanical Engineering
Indian Institute of Technology, Kanpur

August the 11th, 1971

TABLE OF CONTENTS

SYNOPSIS

The present work is an investigation into the dynamic response of a lathe bed. An experimental set-up was designed and fabricated for the purpose of studying the natural frequencies, mode shapes and the response locus of the lathe bed.

Lumped parameter technique is applied for analysing the bed structure. The lathe bed is modelled as a space frame with masses lumped at suitable stations and connected by massless spring elements. The analysis of bed is made (i) with portal and (ii) without portal.

A computer programme is developed for analysis of the bed structure to get the natural frequencies harmonic response locus and the mode shapes.

The dynamic response of the lathe was measured by exciting the structure at the centre by a magnetic shaker. A force dynamometer was placed between the shaker and the structure and the force signal from the dynamometer was displayed on an oscilloscope for measurement. Piezoelectric accelerometers were used as vibration pickups and the signal from the accelerometers were displayed on another oscilloscope for measurement.

The computed and experimental values were compared and a close agreement between the two was observed.

NOTATIONS

$[I]$	-	Unity matrix
$[k^i]$	-	i^{th} element's stiffness matrix in local coordinates
$[\bar{k}^i]$	-	i^{th} element's stiffness matrix in reference coordinates
$[\bar{K}]$	-	Assembled stiffness matrix of structure in reference coordinates
m	-	Total number of elements in structure
$[\bar{m}^i]$	-	i^{th} element's mass matrix in reference coordinates
$[\bar{M}]$	-	Assembled mass matrix of structure in reference coordinates
$[m^i]$	-	i^{th} element's mass matrix in local coordinates
$\{P\}$	-	External load matrix
$\{P_0\}$	-	Generalised load matrix
$\{u^i\}$	-	i^{th} element's displacement matrix in local coordinates
$\{\bar{u}^i\}$	-	i^{th} element's displacement matrix in reference coordinates
$[\bar{U}]$	-	Displacement matrix of complete structure in reference coordinates.
λ_{ox}	-	Direction cosines of ox in reference coordinates
λ_{oy}	-	Direction cosines of oy in reference coordinates
λ_{oz}	-	Direction cosines of oz in reference coordinates
$[\lambda]$	-	i^{th} element's transformation matrix for transforming from local coordinates to reference coordinates
ϕ	-	Phase angle in radians
ω	-	Forcing frequency in radians/sec.
ω_n	-	Natural frequency in radians/sec.
ω_{nj}	-	j^{th} natural frequency in radians/sec.
$[o]$	-	Null matrix.

LIST OF FIGURES

CHAPTER I

INTRODUCTION AND REVIEW OF PREVIOUS WORK

1.1 Introduction :

The demand for better performance of machine tool re-
quires consistent improvements of their structural design. The
design requirements are all the more stringent in the case of
programme controlled machines, where more exacting dynamic per-
formances are required.

Some attempts (Ref. 1) have been made for predicting
the dynamic behaviour of machine tool structures using perspex
model. However very little work has been done in the applica-
tion of theoretical techniques to the actual machine tool struc-
tures (Ref. 2, 3, 4). Very little use has been made of computers
for predicting the dynamic behaviour of machine tool for select-
ing the optimum structural details at the design stage.

Vibrations produced due to variation of cutting force
pose a serious problem in most machine tools specially when large
volume of materials is removed at high cutting speeds. These
vibrations result in poor finish of work as well as rapid tool
failure. In general, machines resist vibrations better if na-
tural frequencies of vibrations are high and has high damping
capacity. The damping of a structure depends on (a) the
materials from which it is built (b) the method of joining va-
rious elements of structure and (c) machine foundations.

The vibrations encountered during operation of machine tools can be classified into three categories, viz. free, forced and self induced vibrations. The free vibrations are caused by mechanical impulse transmitted through the foundation. In fact the free vibrations die away fairly quickly if the damping of the structure is high. Suitable floor mountings can be used to reduce the magnitude of vibrations transmitted through the foundations.

Forced vibrations result from periodic forces either due to unbalanced rotating masses or caused by discontinuous cutting processes, as is the case with milling operation. These vibrations grow to alarming levels when frequency of periodic forces is close to the natural frequency of the structure. These vibrations are dangerous even when first and second harmonics are close to the natural frequency of the structure. Forced vibrations are controlled by using balancing masses and by working at suitable spindle speeds.

The self induced vibrations are due to the ~~vibrations~~ *variations* of the cutting forces caused by the cyclic variation of the cutting parameter. These vibrations are called chatter vibrations. It is usually difficult to eliminate chatter vibrations in a given structure except by reducing the cutting speed.

The self induced vibrations are mainly caused by dynamic instability of a machine tool. The instability comes into picture because of the interaction between the dynamics of

cutting process and dynamic behaviour of machine tool

structure.

1.2 Review of the Previous Work :

Marten (Ref. 5) conducted experiments on actual structure

and reduced scale model and concluded that the two did not give a

close agreement of results. However he was able to spot the weak

points of the structure by experiments on the reduced scale models.

Taylor and Tobias (Ref. 2) used lumped parameter method of

analysis for analysing a milling machine. Further the computed values

were checked by conducting the experiments on the actual machine and

a fairly good agreement of the results was seen.

Taylor (Ref. 3) analysed a planing machine on digital

computer using the lumped parameter technique. Computed values showed

a fairly good agreement with the experimental results.

Gupta (Ref. 4) studied the dynamic response of a lathe bed

using lumped parameter technique. He also carried out experiments to

verify his theoretical analysis. However he did not get sufficient

agreement between the computed and experimental results. Lack of

agreement was attributed to certain difficulties in experimentation

and inaccuracies in modelling the structures.

The present investigation is a follow-up of Gupta's work. The lathe bed analysed by Gupta (Ref. 4) is remodelled by evitably altering the end conditions and a computer programme is developed to calculate natural frequenciesharmonic response locus, and mode shapes of the structure. Experiments are carried out to verify the theoretical analysis.

CHAPTER II

THEORETICAL ANALYSIS

2.1 Introduction :

In this chapter an outline of theoretical analysis is given; which is used for the analysis of the bed of a lathe. The various stages in analysis are :

i) constructing a geometrical configuration of lathe bed;

ii) proposed a model with portrals and a model without portrals;

iii) the coordinate systems;

iv) the mathematical simulation of structure;

v) constructing the mass matrix and stiffness matrix of various elements;

vi) assembly of stiffness and mass matrices of the whole structure;

vii) the equations of motions and response of structure.

2.2 Geometrical Configuration of the Lathe Bed :

The lathe bed is shown in Figure 1 and its photograph in Figure 19. The geometrical details of the bed were taken from Ref. 4. Because of non availability of detailed drawings the bed details were measured by a tape and recorded by Gupta. These dimensions were again checked and found to be correct.

2.3 Proposed Model :

Two models for the lathe bed are proposed. Firstly, the bed with portals removed and secondly the bed with portals. Two models are proposed such that the effect of portrals on the bed behaviour could be observed; both theoretically and experimentally. The proposed models are shown in Figures 1A and 1B.

In the model when portals are removed, the bed is bolted to the foundation by four bolts providing rigidly fixed end condition and in the model the beams are thus taken to be fixed ends.

In the model when portals are there, portral is modelled by four vertical elements at each end and the ends are rigidly fixed to the foundation. Since we are using lumped parameter technique, the masses have been assumed to be lumped at suitable stations. The stations selected are all the joints of rib and the beam and the fixed ends. By having stations as the joints it was possible to have the mass of ribs transferred on to the beams. The stations are connected by massless spring elements.

2.4 The Coordinate Systems :

Two coordinate systems - local coordinate system of individual element and the reference coordinate for the

structure, are used in analysis. The local coordinate system has its origin at one end of the element and the length of element along its x axis. The reference coordinate system has its origin at the lower left corner joint of structure.

The mass and stiffness matrix for each element is first written in local coordinate system and then transformed to the reference coordinate system for assembly.

2.5 The Mathematical Simulation of Structure :

The model with portyal, shown in Figure 1A has 22 station points; and has seven types of elements. The station points can be numbered in an arbitrary faishon, but once numbered the same numbering be referred to every time. The stations are numbered as shown. This pattern is choosen since this gives the assembled mass matrix as diagonal one. The stations points 1, 2, 3, 4 and 19, 20, 21, 22 are completely restrained. The structure is modelled as a space frame, thus each end of an element has 3 rotational and 3 translational degrees of freedom. Thus the total number of degrees of freedom for structure are 132, and of which 48 are restrained.

The model without portyal, shown in Figure 1B has total of 14 station points, from which 1, 2 and 13, 14 are completely restrained. The structure has 84 degrees of freedom out of which 24 are restrained.

2-6 Construction of Mass and Stiffness Matrices :

For constructing the mass and stiffness matrices and then
the equations of motions from them, a few assumptions are made. It
is
is assumed that the bed /made up of a few basic beam elements and
elements are rigidly connected to each other at joints. It is
assumed that the force displacement relations are unique and are
not affected by path of loading the structure or motion causing the
deflected shape. This means that material is ideally elastic over
the range of stress and strain involved in the loading; and the
friction forces in structure and drag forces induced due to move-
ment of structure in ambient fluid, air, are absent. Also the
stress strain relations are considered to be the linear ones i.e.
force and displacements are also linearly related. This allows us
to make use of the superposition principle. This assumption of
linearity is highly idealistic and the force displacement relation-
ship also depends upon geometry and constraints of structure. The
linearity in force deflection relations cannot be postulated in
ideally elastic materials, since the distribution of internal forces
and hence strains change due to change in geometry as load and
deflection are increased. It is also possible that during loading
the system constraint may change thus introducing another source
of non-linearity.

However, we are working under sufficiently small dis-
placements such that the force deflection relations are quite
close to linearity.

The element stiffness matrix is made up of elements which gives the force required in a given degree of freedom to produce a unit deflection in the other given degree of freedom of element. There are well known standard techniques for obtaining the elements of stiffness matrix (Ref. 5) viz. - by inversion of force displacement relations, unit displacement theorem, Castiglano's theorem. A brief outline of the procedure to obtain the stiffness matrix is given in appendix II. The sectional properties of beam required in computation of stiff matrix element are calculated using the procedure given in Ref. (6) and is given in appendix I.

The element mass matrix is made up of mass and inertia terms. The sectional properties of elements are made use of for the calculation of mass. The density for the material is taken from Ref. (4). Reference (5) gives a standard method of obtaining the mass matrix. A brief account of it and of the form of mass matrix is given in appendix III.

2.7 Assembly of Stiffness and Mass Matrices :

The element stiffness and mass matrices obtained are in the elemental coordinate. These are first transformed into the reference coordinate by a suitable transformation defined by

$$\left[\bar{k}^i \right] = \left[\lambda^i \right]^T \left[k^i \right] \left[\lambda^i \right] \tag{1}$$

where $\left[\bar{k}^i \right]$ is the element stiffness matrix in the reference coordinate system, $\left[k^i \right]$ being in local coordinate system and $\left[\lambda^i \right]$ is the

transformation matrix obtained by resolving datum displacements in the local coordinates directions. Appendix (IV) shows that the $[\lambda]$ is made up of direction cosines of the angles between local coordinate and reference coordinate system. The form of $[\lambda]$ is

$$[\lambda] = \begin{bmatrix} \begin{array}{c} \lambda_{ox} \\ \lambda_{oy} \\ \lambda_{oz} \end{array} & 0 & 0 & 0 \\ 0 & \begin{array}{c} \lambda_{ox} \\ \lambda_{oy} \\ \lambda_{oz} \end{array} & 0 & 0 \\ 0 & 0 & \begin{array}{c} \lambda_{ox} \\ \lambda_{oy} \\ \lambda_{oz} \end{array} & 0 \\ 0 & 0 & 0 & \begin{array}{c} \lambda_{ox} \\ \lambda_{oy} \\ \lambda_{oz} \end{array} \end{bmatrix} \qquad (2)$$

where

$$\lambda_{ox} = l_{ox} \quad m_{ox} \quad n_{ox}$$
$$\lambda_{oy} = l_{oy} \quad m_{oy} \quad n_{oy} \qquad (3)$$
$$\lambda_{oz} = l_{oz} \quad m_{oz} \quad n_{oz}$$

and l, m, n are the direction cosines of the local coordinates ox, oy, oz in the reference coordinates ox, oy, oz.

The combined stiffness matrix is reached at by expressing the elemental displacements in terms of displacements of structure

$$[\bar{u}] = [A][U]$$ (4)

in which $[\bar{u}]$ is the elemental displacement in reference coordinate system and $[U]$ is structures displacement in reference coordinates. $[A]$ is square matrix having elements as 0 and 1 and thus relating elemental displacements to structures displacements. If $[P]$ is the generalised load vector, i.e.

$$[P] = [P_1 \ P_2 \ ---- \ P_j \ ---- \ P_m]$$ (5)

where P_j is load in direction of displacement u_j, and writing

$$[\bar{k}] = [\bar{k}^1 \ \bar{k}^2 \ ---- \ \bar{k}^i \ ---- \ \bar{k}^m]$$

where $[\bar{k}]$ is a matrix having $[\bar{k}^i]$ submatrices at its diagonal. Now give a vertual displacement $[\delta u]$ to the system and relating the force and displacements we have (Ref. 5)

$$[P] = [A]^T[\bar{k}][A][U]$$ (6)

Also by force displacement relation

$$[P] = [\bar{k}][U]$$ (7)

Thus $$[\bar{k}] = [A]^T[\bar{k}][A]$$ (8)

Equation 8 gives the combined stiffness matrix. Equation 7 gives a static equilibrium condition when the load matrix $[P]$ includes the reactions as well. Since all these forces are not independent

because of the overall equilibrium of structure, the matrix $[\bar{K}]$ is thus singular. The six dependent equations corresponding to six degrees of freedom of rigid body motion are to be eliminated. This is done by making the six displacement on certain selected point equal to zero and eliminating corresponding rows and columns from the $[\bar{K}]$. This gives the following relation

$$[P]_r = [\bar{T}]_r [U]_r \tag{9}$$

r indicates that these are reduced matrices.

Equation 8 can also be written as

$$[A]^T [\bar{K}][A] = \begin{bmatrix} A_1^T \\ A_2^T \\ A_3^T \\ \vdots \\ A_m^T \end{bmatrix} \begin{bmatrix} \bar{k}^1 & \bar{k}^2 & \bar{k}^3 & \cdots & \bar{k}^m \end{bmatrix} \begin{bmatrix} A_1 \\ A_2 \\ A_3 \\ \vdots \\ A_m \end{bmatrix}$$

$$= \sum_{i=1}^{m} [A^i]^T [\bar{k}^i][A^i] \tag{10}$$

This summation is easier to perform rather than computing the matrix multiplication. The boundary conditions can easily be incorporated here in the assembly. The same is achieved on computer by using a chart called Assembly Control Chart, which is nothing but a simple table giving details of geometry of structure.

The assembly control chart in fact adds up all the elements of elemental stiffness matrix coming on to the particular location in the complete matrix.

Proceeding on the same lines as above the mass matrix is also assembled. First it is converted from local coordinate system to reference coordinate system by $[\lambda]$ as under

$$[\bar{m}] = [\lambda]^T [m][\lambda] \tag{11}$$

and by a similar procedure as in case of stiffness matrix the mass matrix of complete structure is

$$[\bar{M}] = [\Lambda]^T [\bar{m}][\Lambda] \tag{12}$$

Again this assembly can be done by summation and the matrices be reduced as in case of stiffness matrix.

2.8 Equations of Motions

The equations of motion for the structure, when a periodic force of amplitude P_0 and frequency ω is applied, are

$$[\bar{M}][\ddot{x}] + [c][\dot{x}] + [\bar{K}][x] = [P_0] \sin \omega t. \tag{13}$$

where $[C]$ is the damping matrix $[X]$ is the displacement vector. The value of damping constant is taken from Ref. 4 . This value was checked by striking the bed and storing the signal picked by accelerometer on a storage scope. Other investigators have said that the damping is proportional to mass matrix or stiffness matrix or a linear combination of the two (Ref. 2, 3, 7).

To solve equation (13) for response and natural frequencies, we proceed as under (Ref. 5). Define a transformation matrix $[N]$ such that

$$[N] = [M]^{-1/2} \tag{14}$$

and $$[X] = [N][Y] \tag{15}$$

Then the equation of motion can be written as

$$[M][N][\ddot{Y}] + [C][N][\dot{Y}] + [\overline{K}][N][Y] = [P_0]\sin \omega t \tag{16}$$

Premultiply (16) by N^T

$$[N]^T[M][N][\ddot{Y}] + [N]^T[C][N][\dot{Y}] + [N]^T[\overline{K}][N][Y] = [N]^T[P_0]\sin \omega t \tag{17}$$

because (14)

$$[N]^T[M][N] = [I]$$

denoting $[N]^T[C][N]$ by $[A]$, $[N]^T[\overline{K}][N]$ by $[B]$ and $[N]^T[P]$ by $[P_1]$, then we have equation (17) as

$$[I][\ddot{Y}] + [A][\dot{Y}] + [B][Y] = [P_1]\sin \omega t \tag{18}$$

Now we define another matrix transformation, such that

$$[Y] = [R][Z] \tag{19}$$

and $[R]$ is a matrix simultaneously diagonalising $[A]$ and $[B]$ and

$$[R]^T[R] = [I] \tag{20}$$

Equation (18) then changes to

$$[I][R][\ddot{Z}] + [A][R][\dot{Z}] + [B][R][Z] = P_1 \sin \omega t .$$

Premultiplying by $[R_j]^T$ we have

$$[R_j]^T[I][R][\ddot{Z}] + [R_j]^T [A][R][\dot{Z}] + [R_j]^T[B][R][Z] = [R_j]^T[P_1] \sin \omega t$$

$$(21)$$

Since $[A]$ and $[B]$ are simultaneously being diagonalized, hence

$$[I][\ddot{Z}] + [E\sim][\dot{Z}] + [E\sim][Z] = [P] \sin \omega t \qquad (22)$$

where

$$[E\sim] = [R_j]^T[A][R] = \begin{bmatrix} 2 \xi_i \omega_{ni} \end{bmatrix}$$

$$[F\sim] = [R_j]^T[B][R] = \begin{bmatrix} \omega^2_{ni} \end{bmatrix}$$

and $[P] = [R]^T [P_i]$

Since $[F\sim]$ and $[E\sim]$ are diagonal matrices, equation (22) represents a set of uncoupled equations which can be solved for Z.

One of the equation of the set is

$$\ddot{Z}_j + 2\omega_{nj} \dot{Z}_j + \omega^2_{nj} Z_j = P_j \sin \omega t$$

and has a solution as

$$Z_j = \frac{P_j \sin \omega t}{\left[(\omega^2_{nj} - \omega^2)^2 + (4\xi^2_i \omega^2_{nj} \omega^2) \right]^{\frac{1}{2}}} \qquad (23)$$

at a lagging phase of $\emptyset$ given by

$$\emptyset = \tan^{-1} \left(\frac{2\xi_j \omega_{nj} \omega}{\omega^2_{nj} - \omega^2} \right) \qquad (24)$$

Once these values of Z's are obtained these can be substituted

back to get the response in X, by using equation (19) and (14).

2.9 Frequency Computations :

The natural frequencies ω_n are calculated for the system

by obtaining the Eigen values of the matrix $[B]$. The Eigen

values were obtained by Jacobi's method. In this method the

matrix $[B]$ is successively transformed to a diagonal matrix $[D]$

using transformation matrices $[R]$'s such that we have

$$\left[R_n \ R_{n-1} \ R_{n-2} \ \text{---} \ R_2 \ R_1 \right] \left[A \right] \left[R^T \ R_2^T \ R_3^T \ \text{---} \ R_{n-1}^T \ R_n^T \right] = \left[D \right]$$

and then the Eigen values are the diagonal terms of matrix $[D]$.

The Eigen vectors corresponding to these Eigen values are, then

the columns of the matrix $[T]$ given by

$$\left[T \right] = \left[R_1^T \ R_2^T \ R_3^T \ \text{---} \ R_n^T \right]$$

These rotational matrices $[R]$ are formulated on the

basis of eleminating largest off diagonal term (Ref. 8). Since

the Jacobi's method starts with the dominant Eigen value and we

are interested in lowest Eigen value, the matrix $[B]$ is read

in with a negative sign giving us the lowest Eigen value.

CHAPTER 3

EXPERIMENTAL SET - UP AND INSTRUMENTATION

3.1 Introduction :

To verify theoretical analysis the dynamic response of
the structure was experimentally determined taking lathe bed
(i) with portal (ii) and without portal. The experimental set-
up is shown in Figure 2/and the block diagram of instruments is
,18
shown in Figure 4. The lathe bed was excited at the centre/by *(fig.19)*
an electromagnetic shaker and the force and displacement were
measured using a force dynamometer and accelerometer respectively.
The phase difference between force and the displacement was mea-
sured with respect to a standard signal.

3.2 Set - Up and Instrumentation :

The electromagnetic shaker was held over a mild steel
plate which was rigidly fixed to the foundation by six foundation
bolts. The shaker generates a harmonic force signal. The shaker
is connected to the dynamometer by a left hand - right hand bolt(Fig 19)
The electrical power to shaker is given through a suitable power
amplifier. The power amplifier operates on A.C mains.

The force dynamometer (Fig. 3) was connected to shaker
from one side and to the lathe bed from the other by suitable
bolts. The dynamometer was designed for a load level of 50 lbs. *(app.5)*
amplitude of a periodic force, with a natural frequency of
1800 c.p.s. It was expected that in the range of 50 to 600 c.p.s
the dynamometer would give a flat response. The dynamometer is

capable of measuring two forces simultaneously, mutually perpen-
dicular as shown in Figure 3.22. Strain gauges were pasted at
suitable positions on the dynamometer to minimise the cross
response. The dynamometer was calibrated in the two directions
and the cross response was found to be negligibly small. The
output from dynamometer was fed to an amplifier so that the signal
level could be raised to a value suitable for the phase meter.
The output from dynamometer was also displayed on an oscilloscope
for measuring the level of forcing function from shaker.

The lathe bed was excited at the central rib by gripping
central rib in a U bolt. The U bolt was connected to the bolt
from shaker through a suitable plate.

The Endevco accelerometers were used as vibration pick-
ups. Suitable Aluminium blocks *(Fig 21)* were mounted on the lathe bed
and the accelerometers were mounted on these Aluminium blocks.
The output from the accelerometers were amplified on a suitable
amplifier and then displayed on an oscilloscope and was also
fed to the input terminals of a phase meter.

A phase meter was used to measure the phase difference
between the forcing signal from dynamometer and the accelerometer
output. Since the two signals were not upto the required level
for the phase meter, they were compared with another standard
signal of the same frequency and the phase difference was then
computed.

The frequency of excitation was controlled by a frequency generator. The output of frequency generator was fed to the power amplifier supplying power to magnetic shaker.

3.3 Experimental Procedure :

The experiment was first performed without portal with the bed bolted on the foundations. The following procedure was used:

(1) The dynamometer was caliberated using standard weights. The calibration curve is found to be linear and to shown in figure 5.

(2) The function generator was set to give sinusoidal wave form at a particular frequency. The output from function generator and power amplifier were checked on an oscilloscope to ensure that the signal supplied to the shaker in sinusoidal.

(4) The power to the shaker was supplied by the power amplifier and amplitude of the forcing signal was maintained at 7.5 kgs. by adjusting the input current to the shaker.

(5) The signals from the accelcrometers and the dynamometer were measured by displaying them on the oscilloscopes.

(6) The output from the dynamometer was fed to the phase
meter through an amplifier and its inphase and quadrature
components with respect to a reference signal from the
function generator were measured.

(7) The inphase and quadrature components of the signal from
the accelerometer were measured in a similar manner as
under (6) by replacing the dynamometer signal with the
accelerometer signal.

(8) The above procedure was repeated by increasing the
frequencies from 60 to 1000 cps in steps of 10 cps.
Whenever a mode was detected, a number of readings in
that range were were taken at suitable intervals.

(9) The above experiments were repeated by fixing the portals
between the bed and the foundations.

The measured accelerations were converted to displacements by
dividing by ^{2}. The phase between the forcing signal and the displacement
was calculated by taking the difference of phase angle measured under
(6) and (7) and by making appropriate corrections for the fact that the
accelerations signal lags behind the displacement by 180°. The phase
shift in the amplifier used for amplifying the force signal was measured
at various frequencies and is shown in figure 6. The average phase
shift of 6° was also accounted for in calculations.

(6) The output from the dynamometer was fed to the phase
meter through an amplifier and its inphase and quadrature
components with respect to a reference signal from the
function generator were measured.

(7) The inphase and quadrature components of the signal from
the accelerometer were measured in a similar manner as
under (6) by replacing the dynamometer signal with the
accelerometer signal.

(8) The above procedure was repeated by increasing the
frequencies from 60 to 1000 cps in steps of 10 cps.
Whenever a mode was detected, a number of readings in
that range were were taken at suitable intervals.

(9) The above experiments were repeated by fixing the portals
between the bed and the foundations.

The measured accelerations were converted to displacements by
dividing by ^{2}. The phase between the forcing signal and the displacement
was calculated by taking the difference of phase angle measured under
(6) and (7) and by making appropriate corrections for the fact that the
accelerations signal lags behind the displacement by 180°. The phase
shift in the amplifier used for amplifying the force signal was measured
at various frequencies and is shown in figure 6. The average phase
shift of 6° was also accounted for in calculations.

CHAPTER 4

RESULTS AND DISCUSSION

4.1 Results :

The frequency response curves, mode shapes and harmonic response locii have been plotted for computed and experimental values in Figures 7 to 17.

The following constants were used in computation. (Ref. 4)

Youngs Modulus E = 9.6×10^{6} p.s.i

Poisson's Ratio   = 0.27

Damping Coeff.   = 0.0046

For the bed with portal, frequency response curves at central rib have been plotted in Fig. 7, frequency response curves at first rib for experimental and computed values have been plotted in Fig. 8 and the direct harmonic response locus at central rib in vertical direction for experimental and computed values have been plotted in Fig. 9. For the bed without portal, frequency response curves at central rib have been plotted in Fig. 10, frequency response curves at first rib have been plotted in Fig. 11 and the direct harmonic response locii at central rib in vertical direction have been plotted in Fig. 12. The frequency response of foundation has been plotted in Fig. 13. Figures 14 and 15 show the experimental mode shapes without and with the portal, respectively. Figure 16 and 17 show the computed mode shapes without and with the portal, respectively. .

4.2 Discussion :

1. Bed with portal - The frequency response curves in Fig. 7 show three displacement peaks. The peaks occur at 115 c.p.s.

200 c.p.s and 290 c.p.s on computed curve with the major mode being
at 290 c.p.s. and at 95 c.p.s., 130 c.p.s., 180 c.p.s. and 310 c.p.s. on
the experimental curve with the major mode at 180 c.p.s. . The dis-
placement at 310 c.p.s. was measured at a force level of 3.75 kg.
amplitude, since it was not possible to excite the structure at
7.5 kg. amplitude force level in the range of 300 to 400 c.p.s. . The
measured displacement was doubled to correspond to the force level
of 7.5 kg. amplitude. The errors in computed displacements at peak
points are − 45% at 290 c.p.s., 8.45% at 200 c.p.s. and 15.8% at
130 c.p.s.. The percentage errors in the theoretical natural frequen-
cies are 11.1% at 180 c.p.s. in vertical direction, 4.15% at 230 c.p.s.
in transverse direction and 3.53% at 410 c.p.s. for torsional vibra-
tions. The response locus curves (Fig. 8) show three distinct loops
corresponding to three frequencies of peak displacements which is
evident in frequency response curves (Figs. 7, 8, 10 and 11).

2. Bed without portal − Frequency response curves (Fig. 10)
show three displacement peaks. The peaks occur at 335 c.p.s., 230 c.p.s.
and 130 c.p.s. on the experimental curve and at 350 c.p.s., 225 c.p.s.
and 160 c.p.s. on computed curve. The errors in displacement at peak
points are 42% at 350 c.p.s., 14.4% at 230 c.p.s. and 5.5% at 130 c.p.s.
The percentage errors in natural frequencies are 1% at 228 c.p.s.
in vertical direction, 6% at 275 c.p.s. in transverse direction and
2.25% at 450 c.p.s. in torsional vibrations based on the theoretical
values. The response locus curves show three distinct loops

corresponding to peak displacement as shown in frequency response curves also.

Figures 7, 10 and 11 show that computed frequencies are higher than the experimental ones. The lower natural frequencies obtained from experimental data can be explained on the basis of decreased rigidity of the supports at the ends as compared to the theoretically assumed end condition of complete restraint. The loss of rigidity brings down the natural frequencies and experimental values of displacements are larger.

The study of mode shapes (Fig. 14 to 17) reveals that the bed is weak in vertical direction as the first mode is observed in this direction. The second mode corresponds to transverse direction and the third one to torsional vibrations. The effect of portral with bed (Fig. 14 to 17) is to lower the natural frequency due to increased flexibility.

The reasons for discrepancies in displacements and frequencies observed experimentally are :

    i) Flexibility of the exciting system - the exciting system constituting the dynamometer, two bolts, the U bolt and the plate has its own natural frequency which affects the excitation and hence response of the structure.

ii) Flexibility of the supporting system — Due to the flexibility of the supports the boundary conditions considering fixed ends are not strictly true. The flexibility in the transverse direction changes by an appreciable amount due to the bolts at the supports. This lowers the natural frequency affecting largely the first mode. This flexibility also gives rise to rigid body motion, thus affecting the response.

iii) Feed back loop formed through the foundation also changes the dynamic characteristics of the bed.

CHAPTER 5

CONCLUSIONS AND SUGGESTIONS FOR FURTHER WORK

From the results of the present work it is concluded that the lumped parameter technique when applied to the lathe bed can predict the natural frequencies within 10% in the worst case. Furthermore this technique can be used to compare two or more machines for their dynamic behaviour and it can also be used for selecting the best design out of the available sections at the design stage.

For further work it is suggested that the structure be analysed along with mountings on the bed and response at the tool post, head stock and tail stock be measured. It is suggested that a greater number of vibration pick-ups be arranged and used such that the response at a number of places be measured. Filters need to be used with these pick-ups such that low frequency signals and noise can be eliminated. It is suggested that to avoid the feed back loop the structure be excited from the top. Investigations can also be carried out by pre-loading the structure.

It is also suggested that the structure be analysed with a greater number of station points. A further step would be to consider the distributed mass matrix of elements instead of lumped mass system and the damping matrix be estimated theoretically.

REFERENCES

1. R.H. Thornley   —   Machine Tool Structures using model
                            techniques — The Manchester Association
                            of Engineers, Session 1964-5, No. 3.

2. S. Taylor &   —   Lumped Constant Method for the Prediction
    S.A. Tobias   of Vibration Characteristics of Machine
                            Tool Structures — Advances in Machine
                            Tool Design and Research. Sept. 1964, pp. 37.

3. S. Taylor   —   A Computer Analysis of Openside Planing
                            Machine — Advances in Machine Tool
                            Design and Research. Sept. 1965, pp. 197.

4. A.K. Gupta   —   Investigation into the Dynamic Response
                            of Lathe Bed — M. Tech. Thesis — Mech. Engg.
                            Dept. I.I.T.K. 1970.

5. J.S. Prezemiencki —   Theory of Matrix Structural Analysis
                            McGraw Hill Book Co. — 1968.

6. J.C. Maltback   —   Moments of Area Aerofoil Sections,
                            Aircraft Engg., December 1961, pp. 321.

7. S. Taylor   —   Design of Machine Tool Structures using
                            Digital Computers — Advances in Machine
                            Tool Design and Research — Sept. 1966. pp. 369

8. Anthony Ralston —   A First Course in Numerical Analysis
                            McGraw Hill — Kogahusha, 1965

9. W.C. Hurty &   —   Dynamics of Structures, Prentice Hall of India
    M.F. Rubenstein   Pvt. Ltd., 1967

10. M.C. Shaw   —   Metal Cutting Principles, Oxford and I.B.H.
                            Publishing Co. 3rd Edition, 1960

11. B.L. Dhooper   —   Lecture Notes — Intensive Course on Design for
     and N.C. Nigam   Vibration Environment, March 2-11, 1970,
                            I.I.T. Kanpur

12. H.R. Morten   —   Use of Models for Analysis of Machine Tool
                            Structures— Prodn. Engg. — 1962, pp. 63

Evaluation of Sectional Properties :

The section of the element is approximated by straight
line sigments and circular arc segments. The procedure is to cal-
culate the sectional properties under the upper contour and subtract
the same of the lower contour of section. The formulaes for a
straight lines and circular arcs are given as under -

(1) Straight line

$\quad$ Let $\quad a = (x_2 - x_1) \qquad$ (A-1)

$\qquad\quad b = (y_2 - y_1) \qquad$ (A-2)

then $\qquad A = \int\limits_{x_1}^{x_2} y\ dx = (y_1 + \frac{b}{2}) \qquad\qquad$ (A-3)
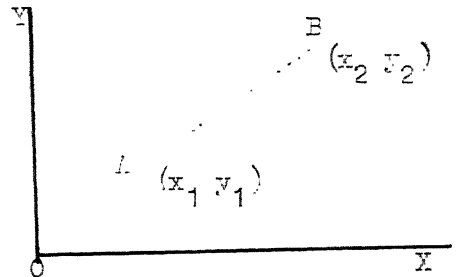
A is the area under line AB. The first moment of inertia and second
moment of inertia about x axis and y axis and product moment of
inertia are given as

$$S_x = \frac{1}{2} \int\limits_{x_1}^{x_2} y^2\ dx = \frac{1}{2}\ a\ (y_1\ (y_1 + b) + \frac{b}{3}) \qquad\qquad \text{(A-4)}$$

$$S_y = \frac{1}{2} \int\limits_{x_1}^{x_2} xy\ dx = a\ (x_1\ (y_1 + \frac{b}{2}) + \frac{1}{2}\ a\ (y_1 + \frac{2}{3}\ b)) \qquad \text{(A-5)}$$

$$I_x = \frac{1}{3} \int\limits_{x_1}^{x_2} y^3\ dx = \frac{1}{3}\ a\ (y_1^2\ (y_1 + \frac{3}{2}\ b) + b^2\ (y_1 + \frac{b}{4})) \qquad \text{(A-6)}$$

$$I_y = \int\limits_{x_1}^{x_2} x^2 y\ dx = a\ (x_1^2\ (y_1 + \frac{b}{2}) + a\ y_1\ (x_1 + \frac{a}{3}) +$$

$$\frac{2}{3}\ b\ a\ (x_1 + \frac{3}{8}\ a)) \qquad\qquad\qquad \text{(A-7)}$$

$$I_{xy} = \frac{1}{2} \int_{x_1}^{x_2} xy^2 \, dx = \frac{1}{2} \, a \, (y_1^2 \, (x_1 + \frac{1}{2} \, a) + b \, x_1$$

$$(y_1 + \frac{b}{3}) + \frac{2}{3} \, ab \, (y_1 + \frac{3}{8} \, b)) \tag{A-8}$$

(2) Circular Arc

Let $\theta_1 = \text{Sin}^{-1} (y_1 - \frac{b}{k})$ (A-9)

$$\theta_2 = \text{Sin}^{-1} (y_2 - \frac{b}{k}) \tag{A-10}$$

Thus for a convex arc $\theta_1 \geqslant \theta_2$

and $0 \leqslant \theta \lesssim \pi$

and for a concave arc $\theta_2 < \theta_1$ and $\pi \leqslant \theta \leqslant 2\pi$

The area A, first moment of section S, and moment of inertia of section about various axes are given by

$$A = \int_{x_1}^{x_2} y \, dx = \frac{R^2}{2} \, (2 \, (\frac{b}{R}) \, (\text{Cos } \theta_2 - \text{Cos } \theta_1) +$$

$$\frac{1}{2} \, (\text{Sin } 2 \, \theta_2 - \text{Sin } 2 \, \theta_1) - (\theta_2 - \theta_1)) \tag{A-10}$$

$$S_x = \frac{1}{2} \int_{x_1}^{x_2} y^2 \, dx = \frac{R^3}{2} \, (((\frac{b}{R})^2 + \frac{3}{4} \, (\text{Cos } \theta_2 - \text{Cos } \theta_1)$$

$$+ \frac{1}{2} \, (\frac{b}{k}) \, (\text{Sin } 2 \, \theta_2 - \text{Sin } 2 \, \theta_1)$$

$$- \frac{1}{12} \, (\text{Cos } 3 \, \theta_2 - \text{Cos } 3 \, \theta_1) - \frac{b}{R} \, (\theta_2 - \theta_1))$$

$$\tag{A-11}$$

$$S_y = \frac{1}{2} \int_{x_1}^{x_2} xy \, dx = R^3 \, ((\frac{a}{R}) \, (\frac{b}{R}) \, (\text{Cos } \theta_2 - \text{Cos } \theta_1)$$

$$- \frac{1}{4} \, (\text{Sin } \theta_2 - \text{Sin } \theta_1) + \frac{1}{4} \, (\frac{b}{R})$$

$$(\text{Cos } 2 \, \theta_2 - \text{Cos } 2 \, \theta_1) \frac{1}{4} \, (\frac{a}{R} \, (\text{Sin } 2 \, \theta_2 - \text{Sin } 2\theta_1)$$

$$+ \frac{1}{12} \, (\text{Sin } 3 \, \theta_2 - \text{Sin } 3 \, \theta_1) - \frac{a}{2R} \, (\theta_2 - \theta_1))$$

$$\tag{A-12}$$

$$I_x = \frac{1}{3} \int_{x_1}^{x_2} y^3 \, dx = R^4 \left(\frac{b}{R} \left(\frac{b^2}{3R^2} + \frac{3}{4} \right) (\cos \theta_2 - \cos \theta_1) \right.$$

$$+ \frac{1}{4} \left(\frac{b^2}{R^2} + \frac{1}{3} \right) (\sin 2 \theta_2 - \sin 2 \theta_1)$$

$$- \frac{b}{12R} (\cos 3 \theta_2 - \cos 3 \theta_1) - \frac{1}{96}$$

$$(\sin 4 \theta_2 - \sin 4 \theta_1) - \frac{1}{2} \left(\frac{b^2}{R^2} + \frac{1}{4} \right)$$

$$\left. (\theta_2 - \theta_1) \right) \tag{A-13}$$

$$I_y = \int_{x_1}^{x_2} y \, x^2 \, dx = R^4 \left(\frac{b}{R} \left(\frac{a^2}{R^2} + \frac{1}{4} \right) (\cos \theta_2 - \cos \theta_1) \right.$$

$$- \frac{1}{2} \left(\frac{a}{R} \left((\sin \theta_2 - \sin \theta_1) + \frac{a}{2R} \left(\frac{b}{R} \right. \right. \right.$$

$$(\cos 2 \theta_2 - \cos 2 \theta_1) + \frac{1}{4} \frac{a^2}{R^2} (\sin 2 \theta_2 -$$

$$\sin 2 \theta_1) + \frac{b}{12R} (\cos 3 \theta_2 - \cos 3 \theta_1)$$

$$+ \frac{1}{4} \frac{a^2}{R^2} (\sin 2 \theta_2 - \sin 2 \theta_1) + \frac{b}{12 R}$$

$$(\cos 3 \theta_2 - \cos 3 \theta_1) + \frac{a}{6R} (\sin 3 \theta_2$$

$$- \sin 3 \theta_1) + \frac{1}{32} (\sin 4 \theta_2 - \sin 4 \theta_1)$$

$$\left. - \left(\frac{a^2}{2R^2} + \frac{1}{8} \right) (\theta_2 - \theta_1) \right) \tag{A-14}$$

$$I_{xy} = \frac{1}{2} \int_{x_1}^{x_2} x y^2 \, dx = R^4 \left(\frac{a}{2R} \left(\frac{b^2}{R^2} + \frac{3}{4} \right) (\cos \theta_2 - \cos \theta_1 \right.$$

$$- \frac{b}{4R} (\sin \theta_2 - \sin \theta_1) + \frac{1}{8} \left(\frac{b^2}{R^2} + \frac{1}{2} \right)$$

$$(\cos 2 \theta_2 - \cos 2 \theta_1) + \frac{1}{4} \frac{ab}{R^2}$$

$$(\sin 2 \theta_2 - \sin 2 \theta_1) - \frac{a}{24R} (\cos 3 \theta_2$$

$$- \cos 3 \theta_1) + \frac{b}{12R} (\sin 3 \theta_2 - \sin 3 \theta_1)$$

$$- \frac{1}{64} (\cos 4 \theta_2 - \cos 4 \theta_1) - \frac{ba}{2R^2}$$

$$\left. (\theta_2 - \theta_1) \right) \tag{A-15}$$

If the superscript 1 denotes the upper boundary and 2 denotes the lower boundary of section thus for section we have

$$A = A^{(1)} - A^{(2)}$$

$$S_x = S_x^{(1)} - S_x^{(2)}$$

$$S_y = S_y^{(1)} - S_y^{(2)}$$

$$I_x = I_x^{(1)} - I_x^{(2)}$$

$$I_y = I_x^{(1)} - I_x^{(2)}$$

$$I_{xy} = I_{xy}^{(1)} - I_{xy}^{(2)} \qquad (A-16)$$

Transformation to principal axes :

The angle of rotation of coordinates is given by

$$\theta = \frac{1}{2} \tan^{-1} \left(\frac{2 I_x' I_y'}{I_y' - I_x'} \right) \qquad (A-17)$$

where I_x' and I_y' are given by

$$I_x' = I_x \cos^2 \theta + I_y \sin 2\theta - I_{xy} \sin 2\theta \qquad (A-18)$$

$$I_y' = I_x \sin^2 \theta + I_y \cos^2 \theta + I_{xy} \sin 2\theta \qquad (A-19)$$

Inertia Properties :

The mass moment of inertia of the elements are obtained by relation

$$I_{mxx} = \rho \int (x^2 + y^2) \, dx \cdot dy \cdot dz$$

$$= \int z^2 \, dy \cdot dz \cdot dx + \int y^2 \, dy \cdot dz \cdot dx$$

$$= \rho \left(\frac{I_y}{2} + \frac{I_z}{2} \right) = \frac{\rho}{2} \left(I_y + I_z \right) \qquad (A\text{-}20)$$

where ρ = mass/unit volume = specific weight $/ g$.

$$I_{myy} = \rho \int (z^2 + x^2) \, dx \cdot dy \cdot dz$$

$$= \rho \left(\frac{I_y}{z} + \frac{A \, l^3}{24} \right) = \frac{\rho}{2} \left(I_y + \frac{A \, l^3}{12} \right) \qquad (A\text{-}21)$$

$$\text{and } I_{mzz} = \rho \int (x^2 + y^2) \, dx \cdot dy \cdot dz$$

$$= \rho \left(\frac{I_z}{z} + \frac{A \, l^3}{24} \right) = \frac{\rho}{2} \left(I_z + \frac{A \, l^3}{12} \right) \qquad (A\text{-}22)$$

Stiffness Matrix :

The complete derivation of stiffness matrix is given in reference 5.

The element k_{ij} of stiffness matrix is defined as "the force required in the direction j to produce a unit deflection in the direction i."

Neglecting shear deformations, rotary inertia effects and thermal loading effects the stiffness matrix for i^{th} element is given by :

$$[k^{(i)}] = \begin{bmatrix}
\frac{EA}{1} & & & & & & & & & & & \\
0 & \frac{12EI_z}{1^3} & & & & & & & & & & \\
0 & 0 & 12\,EI_y/1^3 & & & & \text{Symmetric} & & & & & \\
0 & 0 & 0 & \frac{GJ}{1} & & & & & & & & \\
0 & 0 & -\frac{6EI_y}{1^2} & 0 & \frac{4EI_y}{1} & & & & & & & \\
0 & \frac{6EI_z}{1^2} & 0 & 0 & 0 & \frac{4EI_z}{1} & & & & & & \\
-\frac{EA}{1} & 0 & 0 & 0 & 0 & 0 & \frac{AE}{1} & & & & & \\
0 & \frac{-12EI_z}{1^3} & 0 & 0 & 0 & \frac{-6EI_z}{1^2} & 0 & \frac{12EI_z}{1^3} & & & & \\
0 & 0 & \frac{-12EI_y}{1^3} & 0 & \frac{6EI_z}{1^2} & 0 & 0 & 0 & \frac{12EI_y}{1^3} & & & \\
0 & 0 & 0 & \frac{-GJ}{1} & 0 & 0 & 0 & 0 & 0 & \frac{GJ}{1} & & \\
0 & 0 & \frac{-6EI_y}{1^2} & 0 & \frac{2EI_y}{1} & 0 & 0 & 0 & \frac{6EI_y}{1^2} & 0 & \frac{4EI_y}{1} & 4 \\
0 & \frac{6EI_z}{1^2} & 0 & 0 & 0 & \frac{2EI_z}{1} & 0 & \frac{-6EI_z}{1^2} & 0 & 0 & 0 &
\end{bmatrix}$$

APPENDIX 3

Mass Matrix :

       The complete derivation of mass matrix is given in reference 5. The elemental mass matrix for the lumped parameter model is given by :

$$[m] = \begin{bmatrix} m_1 & & & & & & & & & & \\ & m_1 & & & & & & & & & \\ & & I_{mxx} & & & & & & & & \\ & & & I_{myy} & & & & & & & \\ & & & & I_{mzz} & & & & & & \\ & 0 & & & & m_1 & & & 0 & & \\ & & & & & & m_1 & & & & \\ & & & & & & & m_1 & & & \\ & & & & & & & & I_{mxx} & & \\ & & & & & & & & & I_{myy} & \\ & & & & & & & & & & I_{mzz} \end{bmatrix}$$

Direction Cosine Matrix :
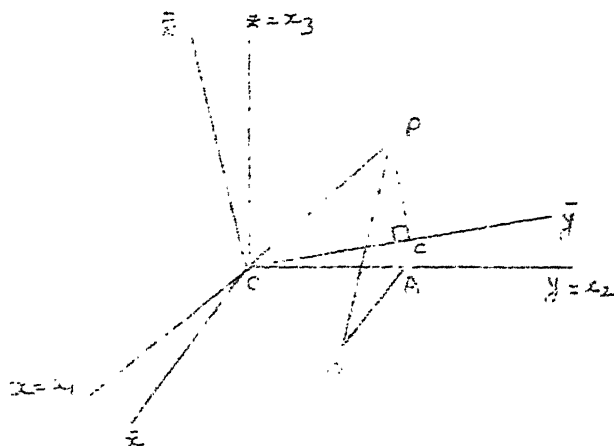
A point P in space has coordinates (x, y, z) along ox, oy, oz. For the new axes, $o\bar{x}$, $o\bar{y}$, $o\bar{z}$, the coordinates of point are $(\bar{x}, \bar{y}, \bar{z})$.

To relate (x, y, z) and $(\bar{x}, \bar{y}, \bar{z})$, we have

$$\bar{x}_1 = l_{11}\, x_1 + l_{12}\, x_2 + l_{13}\, x_3$$

$$\bar{x}_2 = l_{21}\, x_1 + l_{22}\, x_2 + l_{33}\, x_3$$

$$\bar{x}_3 = l_{31}\, x_1 + l_{32}\, x_2 + l_{33}\, x_3$$

where $l_{ij} = \mathrm{Cos}\,(\widehat{x_i\, x_j})$, the direction cosines.

Expressing in matrix notation

$$[\bar{x}] = [\lambda][x]$$

where

$$[\bar{x}] = \begin{bmatrix} \bar{x}_1 \\ \bar{x}_2 \\ \bar{x}_3 \end{bmatrix} \qquad [x] = \begin{bmatrix} x_1 \\ x_2 \\ x_3 \end{bmatrix}$$

and $[\lambda] = \begin{bmatrix} l_{11} & l_{12} & l_{13} \\ l_{21} & l_{22} & l_{23} \\ l_{31} & l_{32} & l_{33} \end{bmatrix}$

Transformation of Elemental Matrix from Local Coordinates to
Reference Coordinates :

The displacements in local and reference coordinates are
related by

$$[u] = [\lambda][\bar{u}]$$

Introducing a virtual displacement, $\bar{u}$ in reference coordinates
can be written in terms of u as

$$\{\delta u\} = [\lambda][\delta \bar{u}]$$

If the loading vector is P on local coordinates and $\bar{P}$ in
the reference coordinates the Equating Virtual Work in reference
and local coordinates we have

$$[\delta \bar{u}]^T [\bar{P}] = [\delta u]^T [P]$$

$$[\delta \bar{u}]^T [\bar{P}] - [\delta u]^T [P] = [0]$$

$$[\delta \bar{u}]^T [\bar{P}] - [\delta \bar{u}]^T [\lambda]^T [P] = [0]$$

or $$[\bar{P}] = [\lambda]^T [P]$$

Since $$[P] = [k^i][u]$$

and $$[\bar{P}] = [\bar{k}^i][\bar{u}]$$

Hence $$[\bar{k}^i][\bar{u}] = [\lambda]^T [k^i][u]$$

$$[\bar{k}^i][\bar{u}] = [\lambda]^T [k^i][\lambda][\bar{u}]$$

or $$[\bar{k}^i] = [\lambda]^T [k^i][\lambda]$$

APPENDIX 5

DYNAMOMETER DESIGN :

The two force dynamometer design is based on expressions
given in reference (10). The criteria for design is the natural
frequency of the dynamometer which should be 4 to 5 times the fre-
quency of forces to be measured, so that the recorded force is not
influenced by any vibrating motion of the dynamometer. For the
analysis purpose the dynamometer is reduced to a mass, m, supported
by a spring. The natural frequency ω_n of such a system is given
by

$$\omega_n = \frac{1}{2\pi} \sqrt{\frac{K}{m}} \quad c.p.s$$

where k is the stiffness of spring.

In terms of weight of dynamometer W

$$\omega_n = \frac{1}{2\pi} \sqrt{386 \frac{K}{W}} \quad c.p.s$$

K is in lbs./in. and W in lbs.

The stiffness of dynamometer in radial direction and tangential
direction are

$$K_r = \frac{E b t^3}{1.8 r^3}$$

and

$$K_t = \frac{E b t^3}{3.6 r^3}$$

where E is the modulus of elasticity of material of dynamometer,

b is the width, t is the minimum thickness and r is the radius of ring.

The strains encountered are given by

$$\epsilon_A = \pm \frac{10.9 \ F_r \cdot r}{Ebt^2}$$

$$\epsilon_A = \pm \frac{218 \ F_t \cdot r}{Ebt^2}$$

The above equations were used for getting the various dimensions

of the dynamometer.

LATHE BED

(A) MODEL WITH PORTAL

(B) MODEL WITHOUT PORTAL

THE LATHE BED AND ITS MODELS   FIGURE #1

LATHE BED

7/8 DIA BOLT

1/2 L BOLT

7/8 LOCK NUT

FOUNDATION
LTS.

3/8 FOUNDATION
BOLTS

7/8 LEFT-HAND
RIGHT-HAND
BOLT

FORCE DYNAMOMETER

MAGNETIC
SHAKER

1/2 STUD

3/8 FOUNDATION BOLTS

REINFORCED CONCRETE FOUNDATION
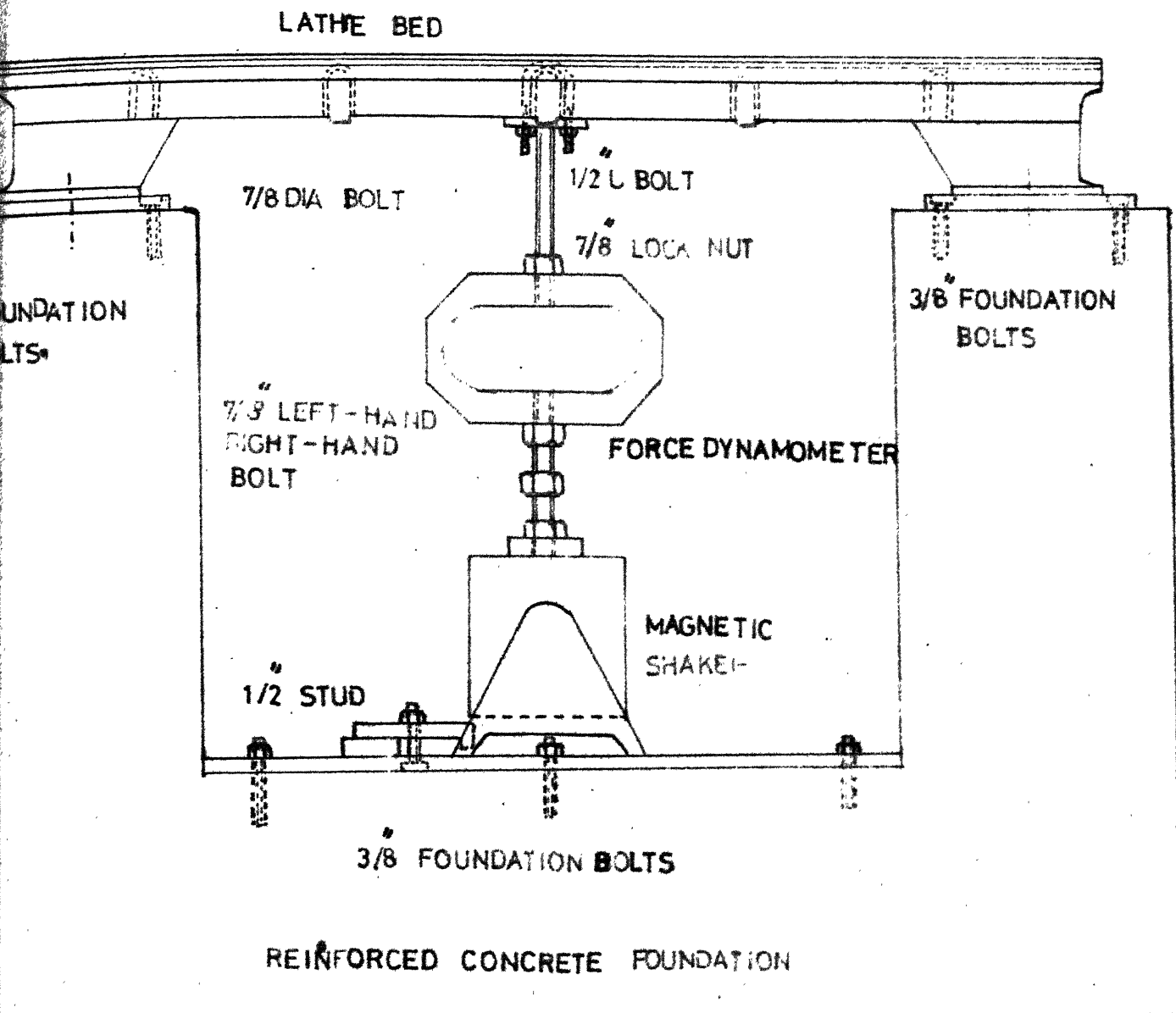
EXPERIMENTAL SET UP

FIGURE # 2

SECTION AT A-A
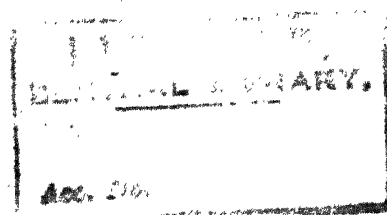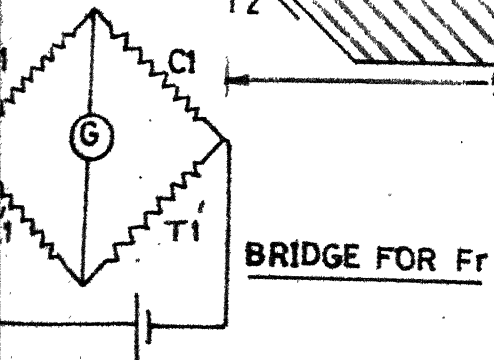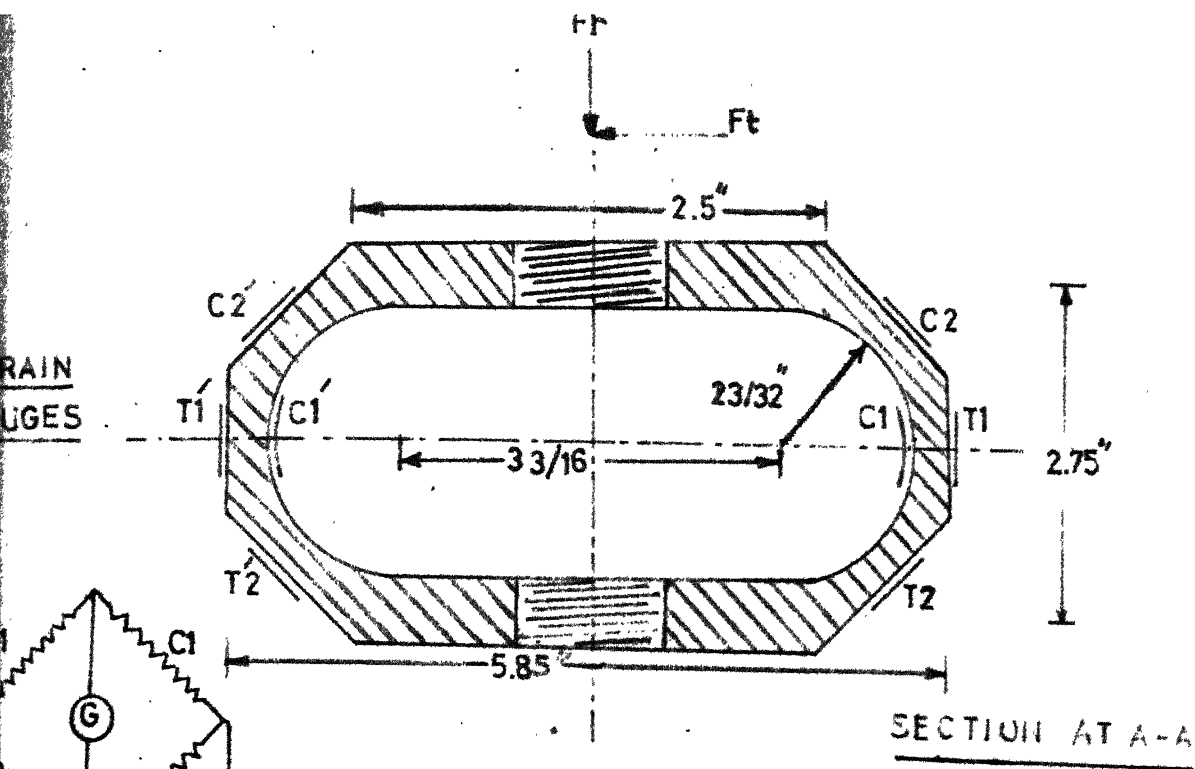
BRIDGE FOR Fr
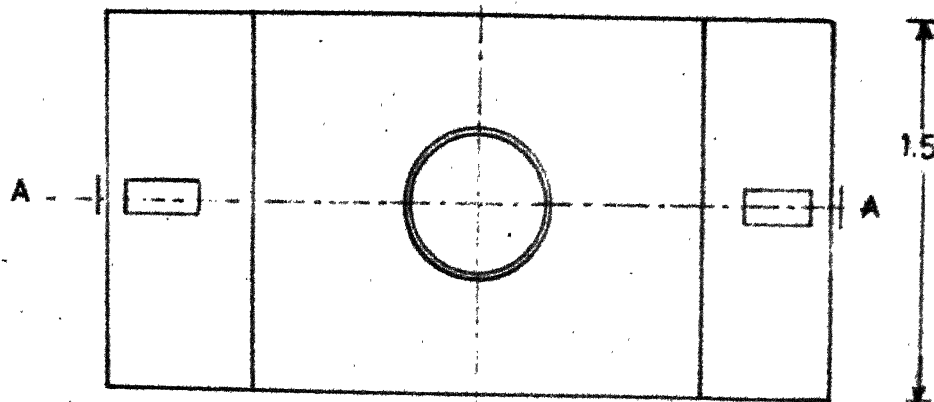
BRIDGE FOR Ft

TWO DIRECTIONAL FORCE DYNAMOMETER

FIGURE # 3

230 VAC 1∅ 50C/S

```
┌──────────────┐
│ FUNCTION     │
│ GENERATOR    │
└──────────────┘
       ┊
       ▼
┌──────────────┐          ┌──────────────┐
│ POWER AMPL-  │          │ LATHE BED    │
│ IFIER        │          │              │
└──────────────┘ ◄─230VAC └──────────────┘
       ┊           1∅50 C/S
       ▼
┌──────────────┐     ┌──────────┐   ┌──────────────┐
│ MAGNETIC     │     │ DYNAMO-  │   │ ACCEROMETERS │
│ SHAKER       │     │ METER    │   │              │
└──────────────┘     └──────────┘   └──────────────┘
              BATTERY
              ─9VDC
┌──────────────┐
│ AMPLIFIER    │
└──────────────┘
```

230 VAC 1∅ 50 C/S

BATTERY ─9VDC

230VAC 50C/S 1∅

┌──────────────┐
│ AMPLIFIER   │   230VAC
└──────────────┘   1∅50 C/S

┌──────────────┐
│ PHASE METER │ ◄─── 230VAC 1∅ 50 C/S
└──────────────┘
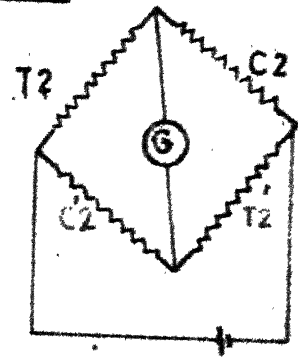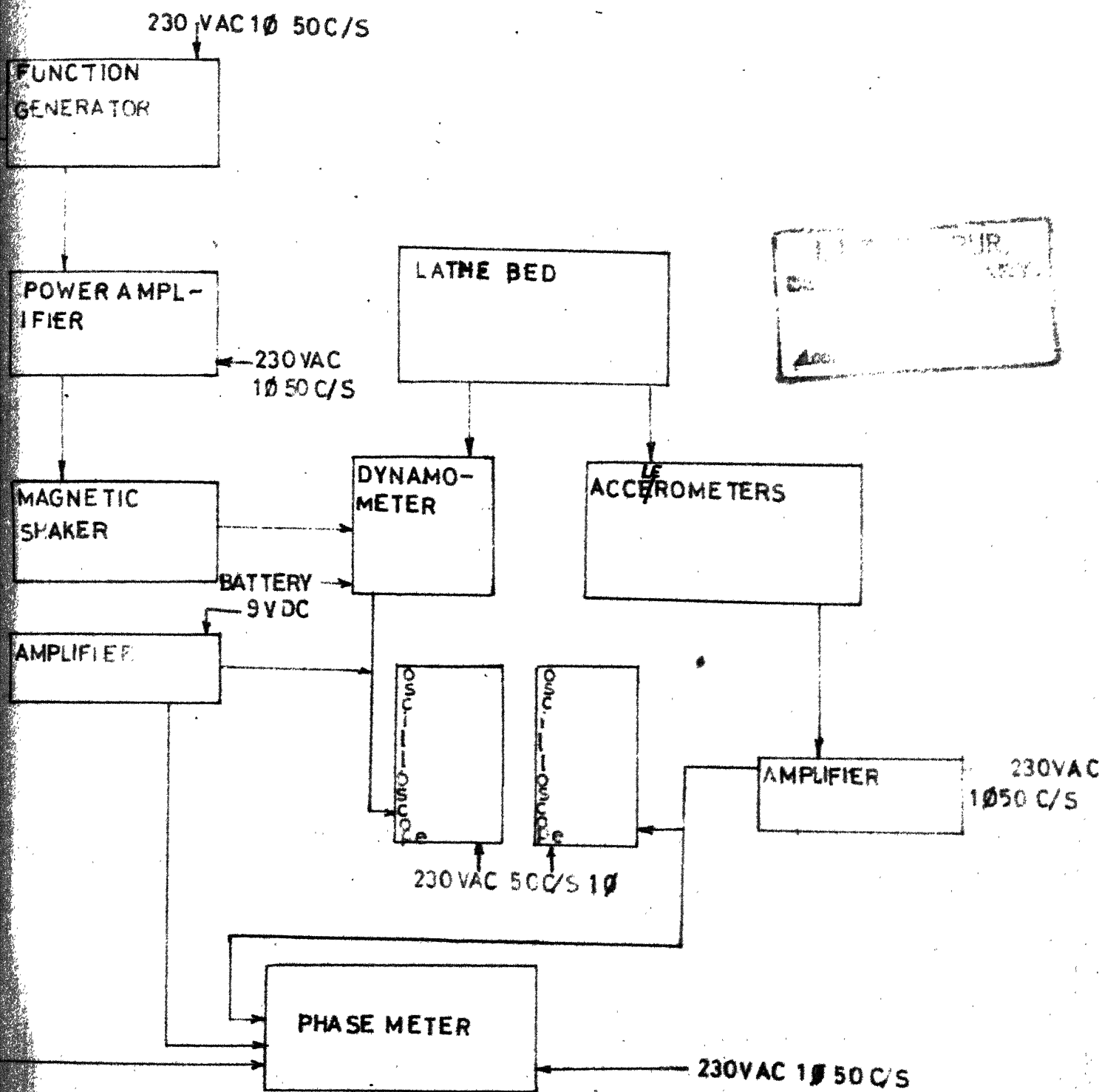
BLOCK DIAGRAM

FIGURE # 4

DYNAMOMETER
CALIBERATION CURVE

BATTERY VOLTAGE = 7.4 V.

LOAD IN KGMS.
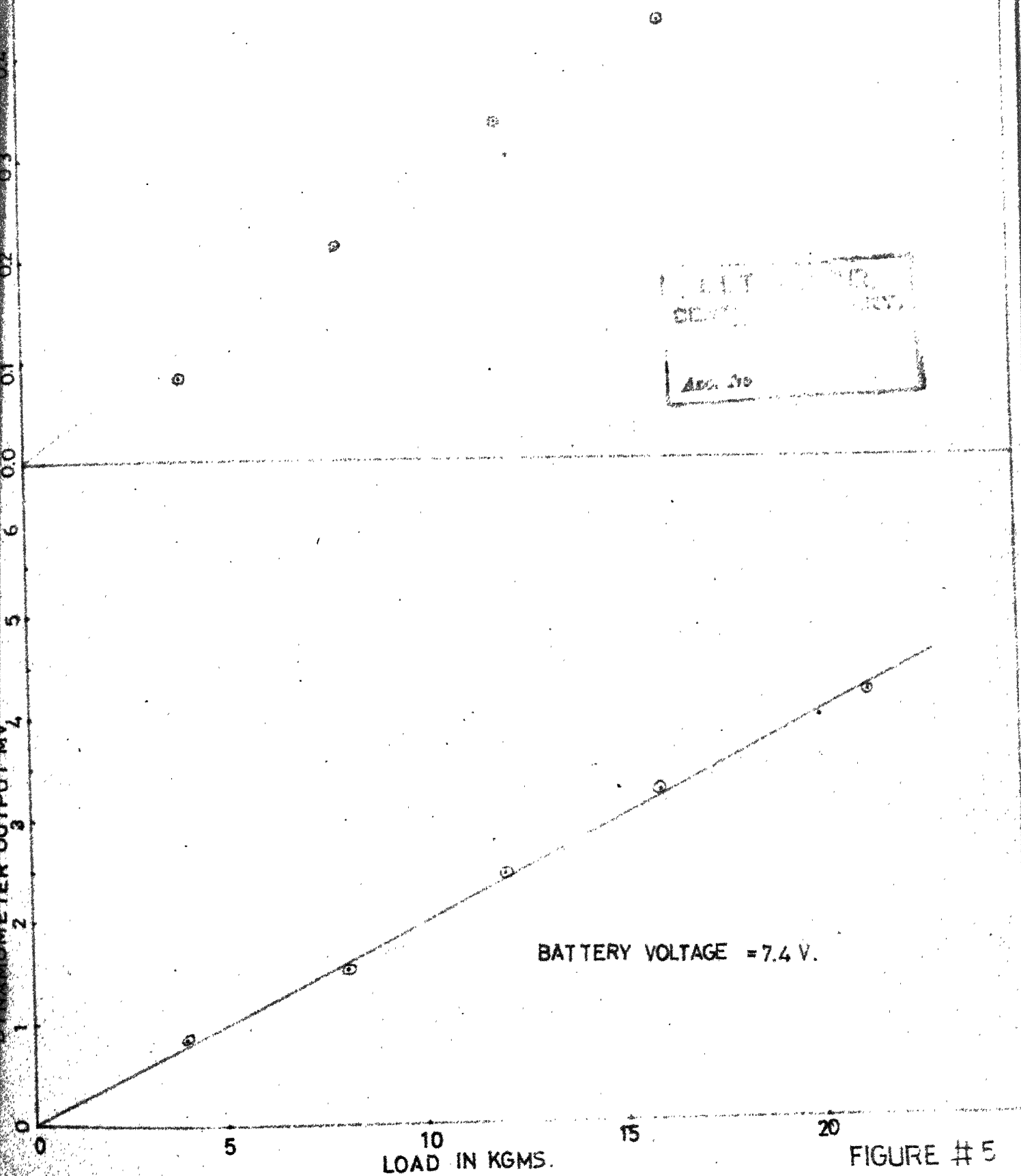
FIGURE # 5

AMPLIFIER PHASE SHIFT PLOT
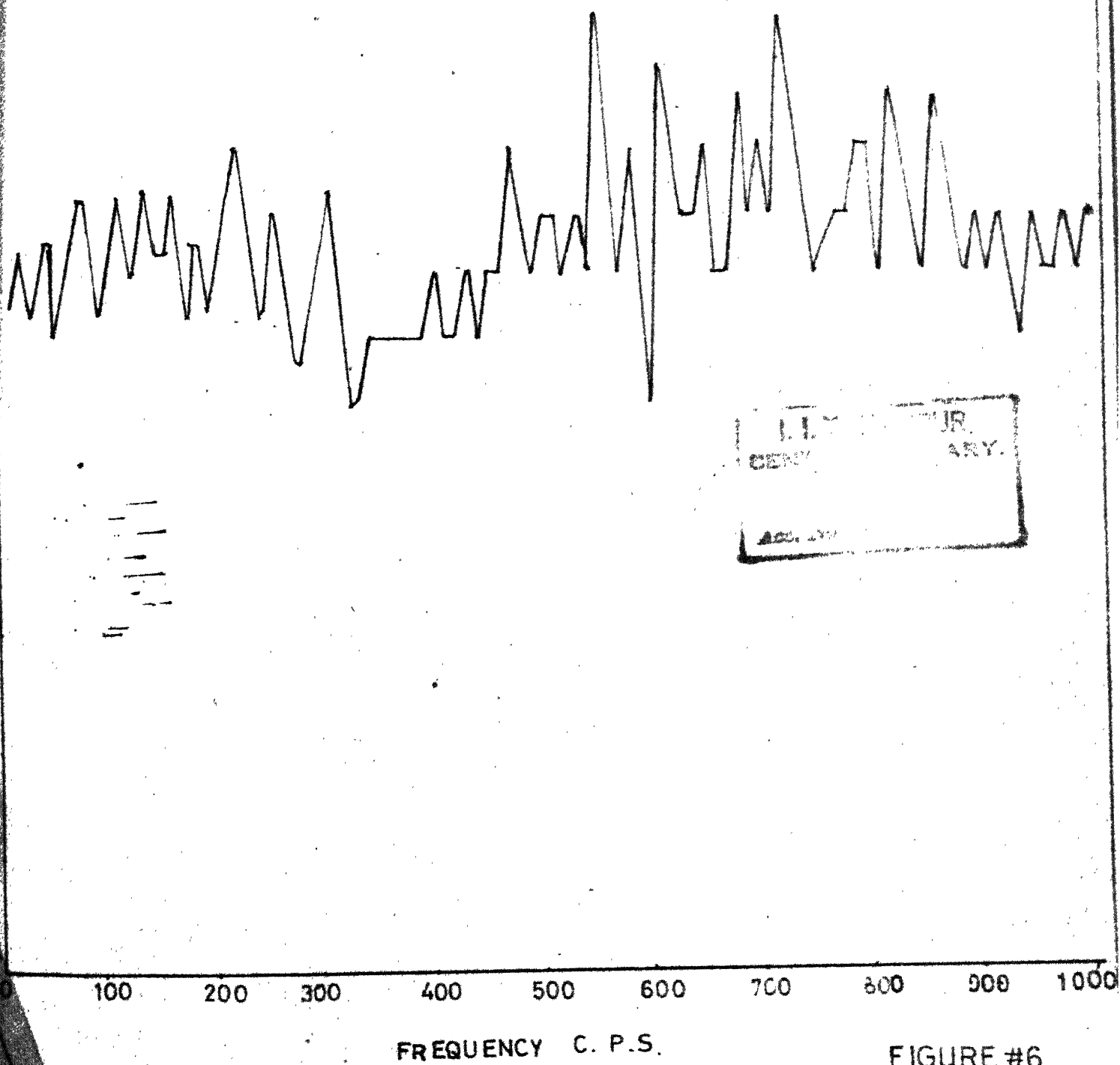
FREQUENCY C. P.S.

FIGURE #6

FORCING FUNCTION
NATURE - SINUSOIDAL
AMPLITUDE - 7.5 KG.

FREQUENCY IN C.P.S.
— EXPERIMENTAL
--- COMPUTED
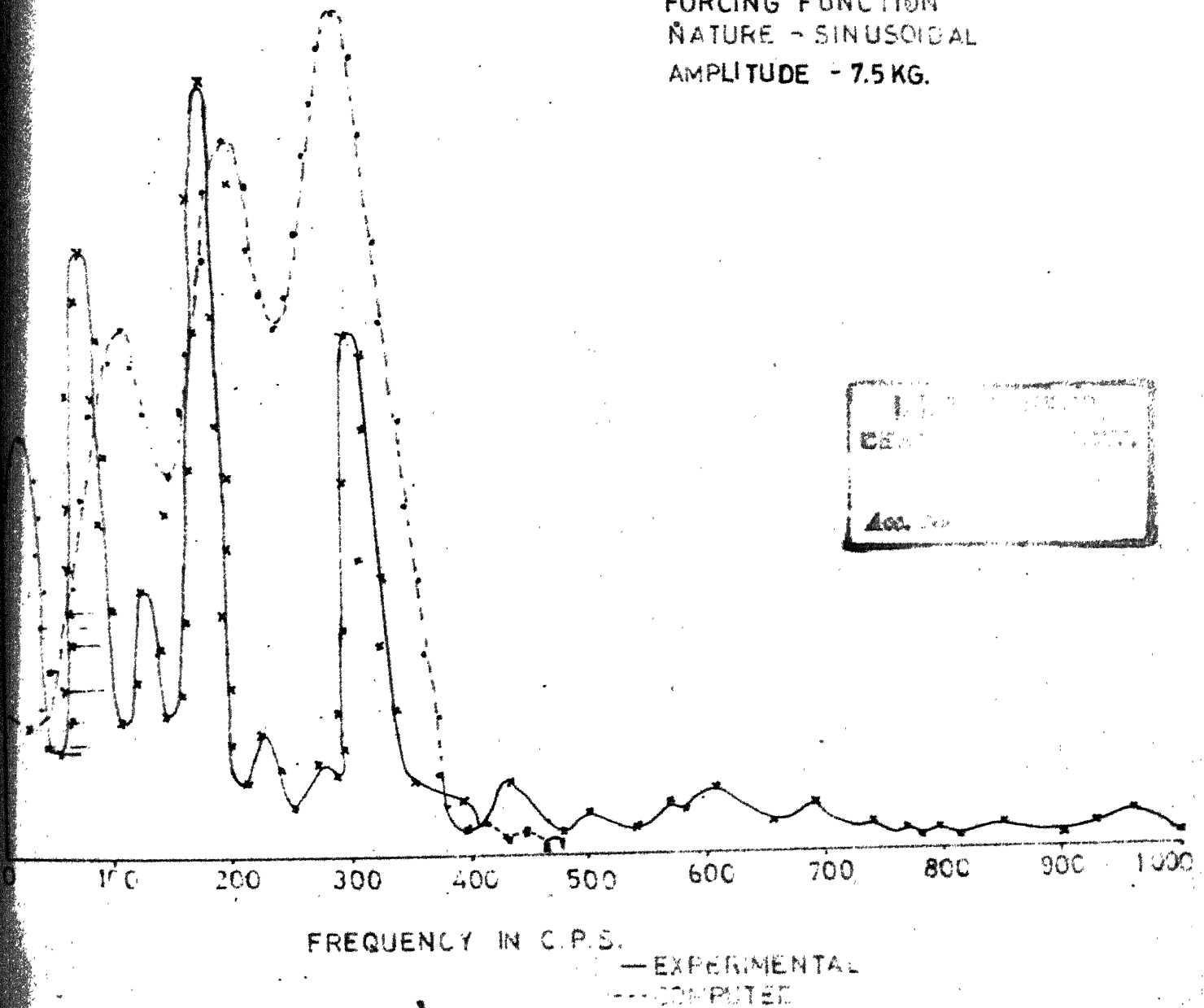
FREQUENCY RESPONSE CURVE
AT CENTRAL RIB WITH PORTAL

FIGURE # 7

FORCING FUNCTION
NATURE – SINUSOIDAL
AMPLITUDE – 7.5KG.
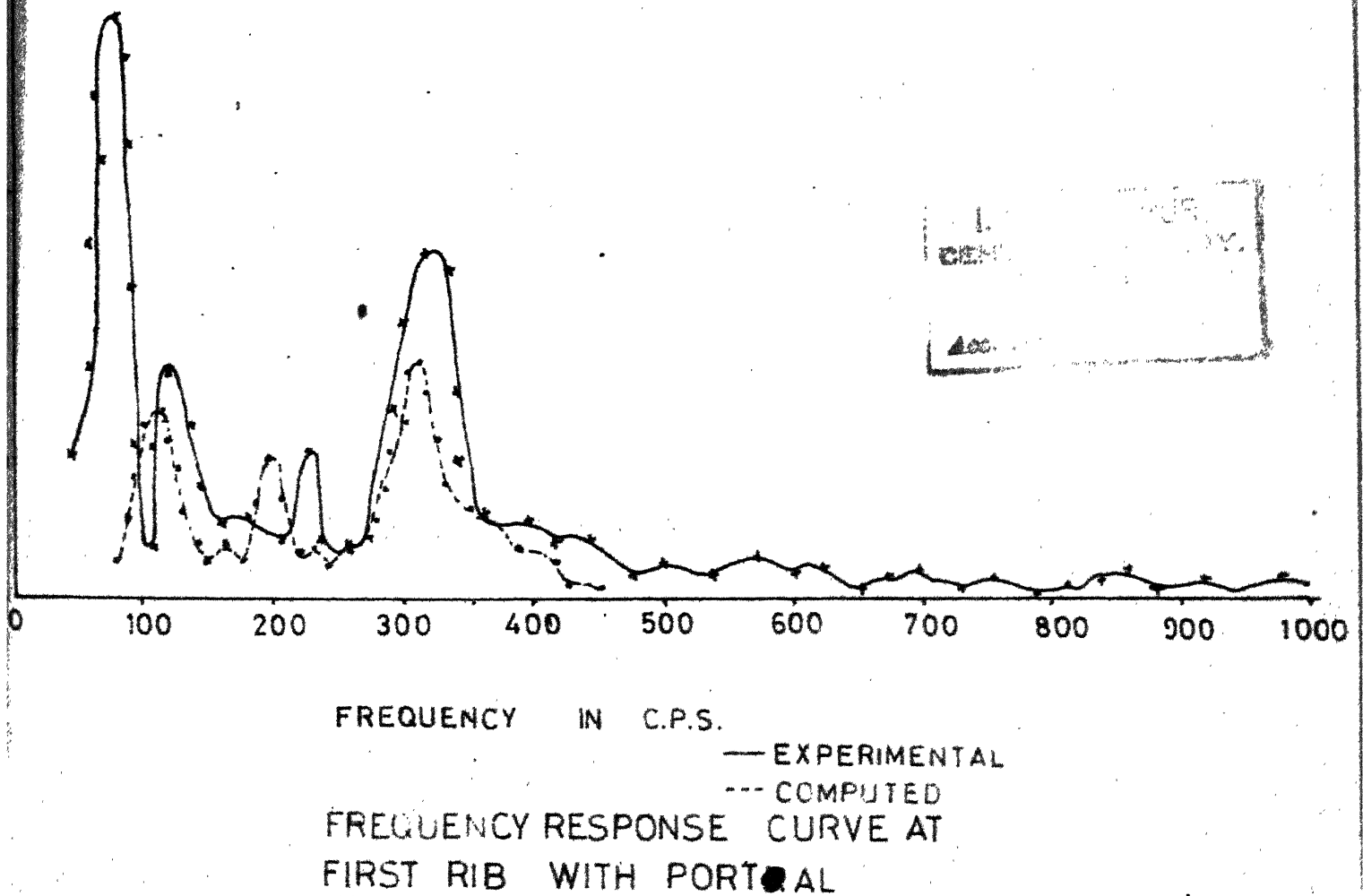
FREQUENCY   IN   C.P.S.

—— EXPERIMENTAL
--- COMPUTED

FREQUENCY RESPONSE CURVE AT
FIRST RIB   WITH PORT●AL

FIGURE#8

COMPUTED
SCALE 1CM = 2×10^{-3} CM

EXPERIMENTAL
SCALE 1 CM. = 2×10^{-3} CM.
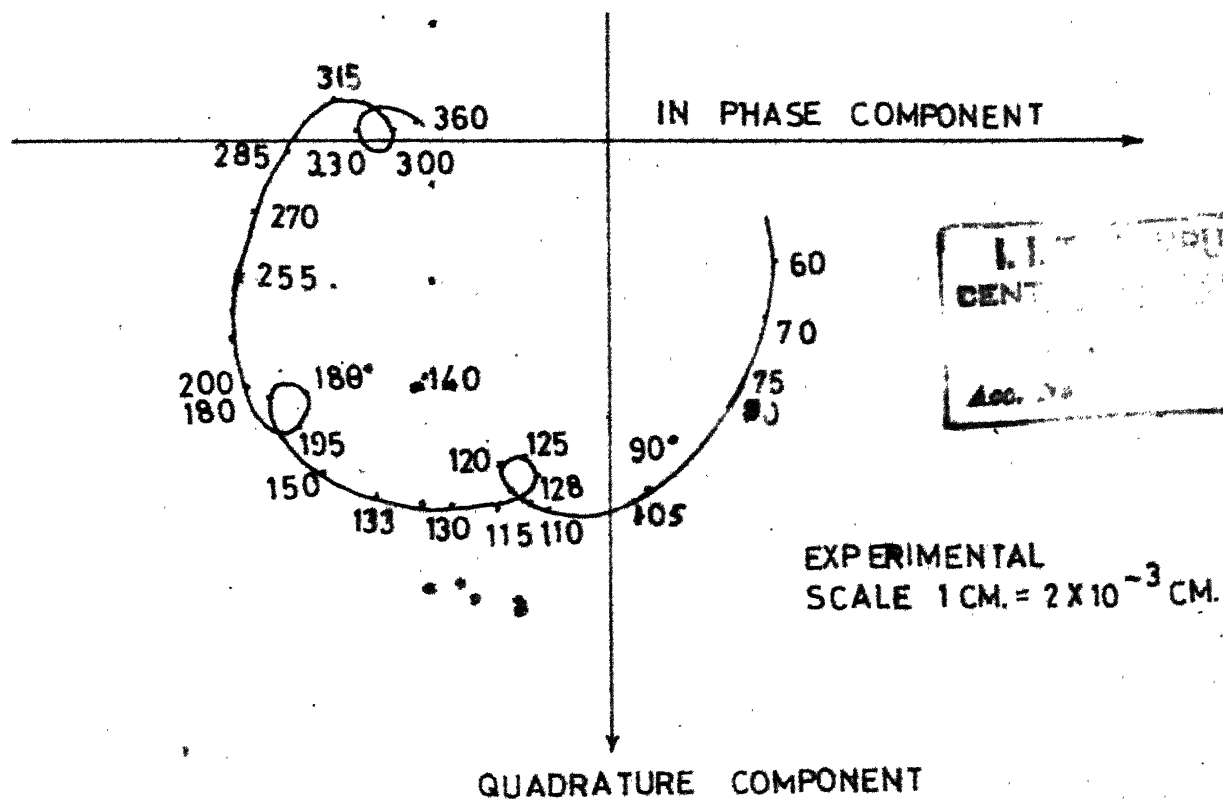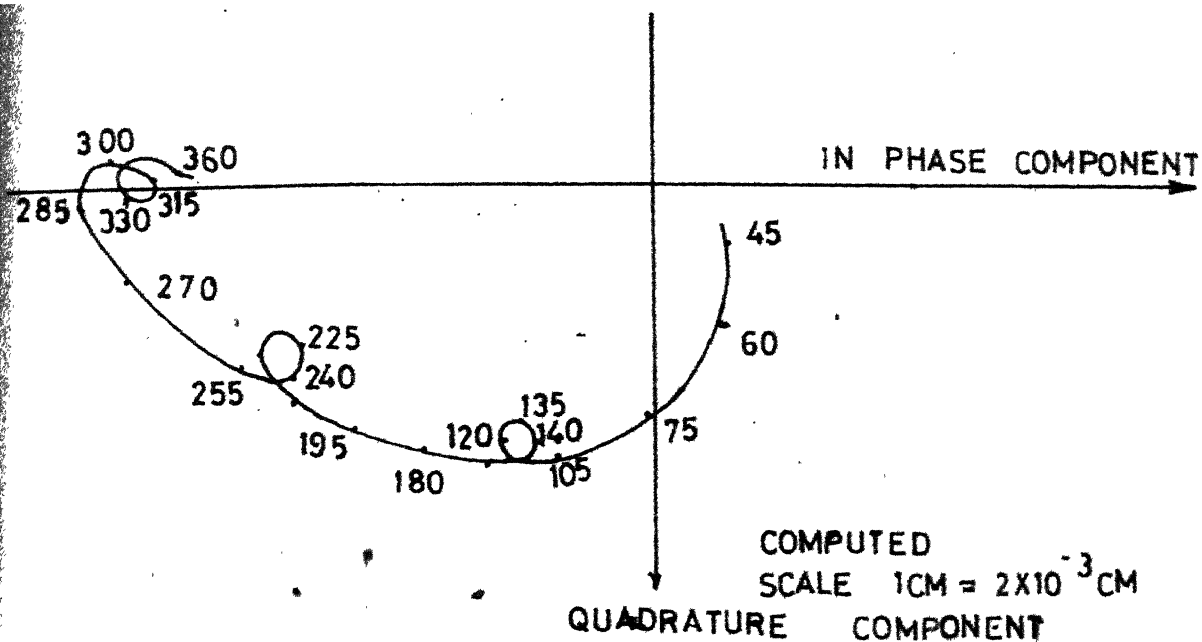
DIRECT HARMONIC RESPONSE LOCUS
IN VERTICAL DIRECTION AT CENTRAL
RIB   WITH PORTAL

FIGURE # 9

FORCING FUNCTION
NATURE - SINUSOIDAL
AMPLITUDE - 7.5 KG.
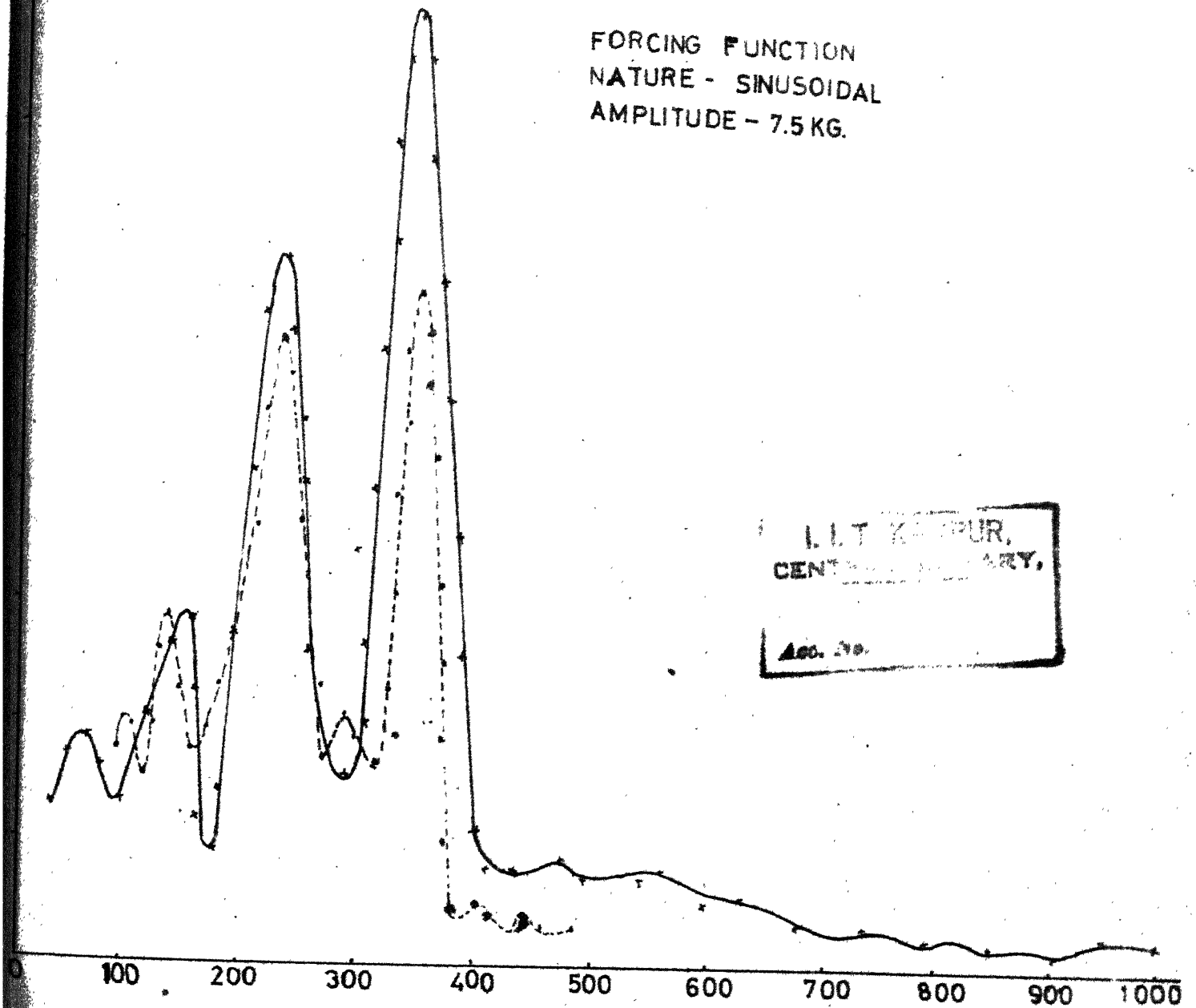
FREQUENCY C.P.S.

—— EXPERIMENTAL
--- COMPUTED

FREQUENCY RESPONSE CURVE AT
CENTRAL RIB WITHOUT PORTAL

FIGURE#10

FREQUENCY RESPONSE
CURVE AT FIRST RIB
WITHOUT PORTAL
FORCING FUNCTION
NATURE – SINUSOIDAL
AMPLITUDE – 7.5 KG
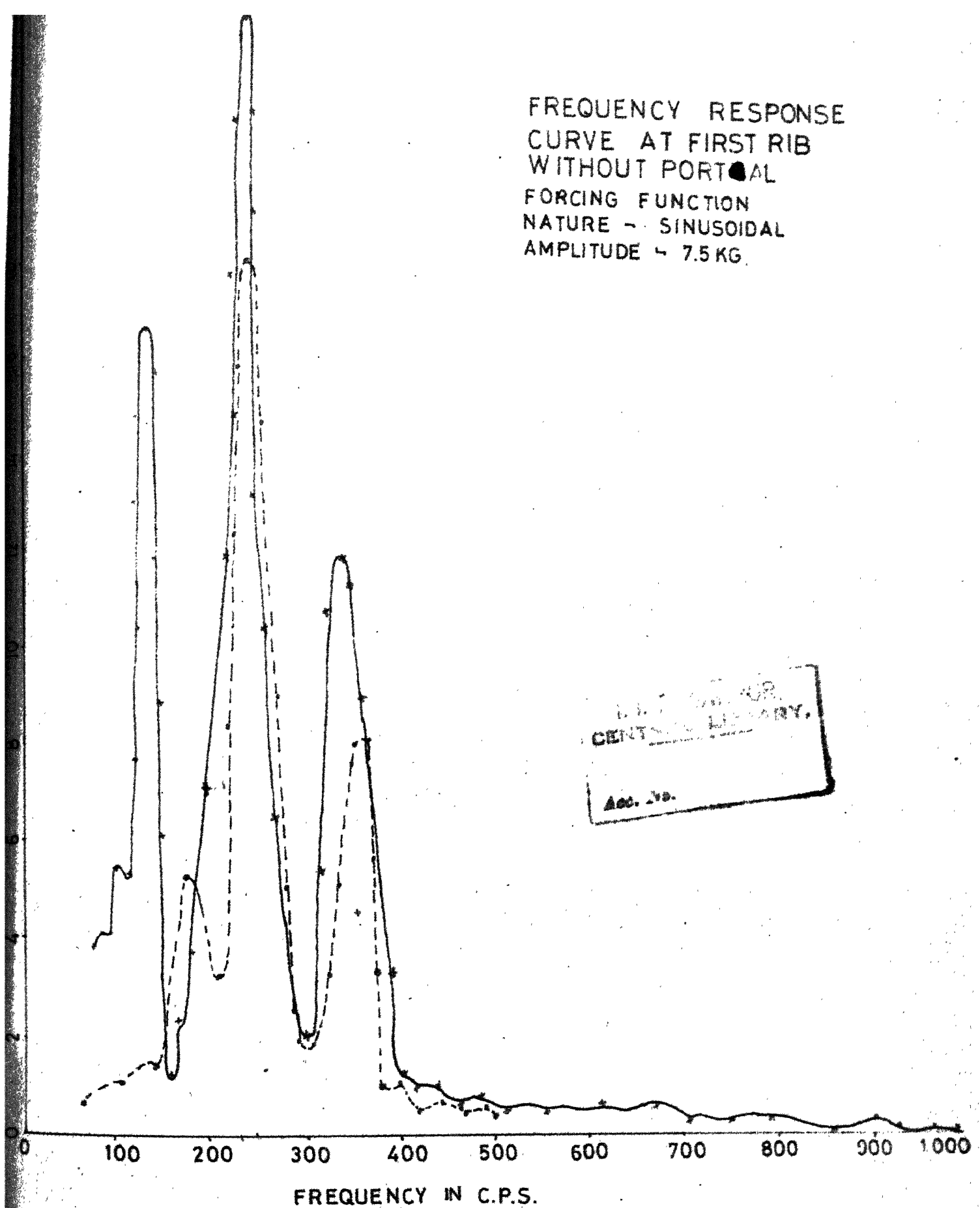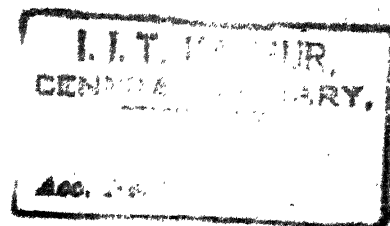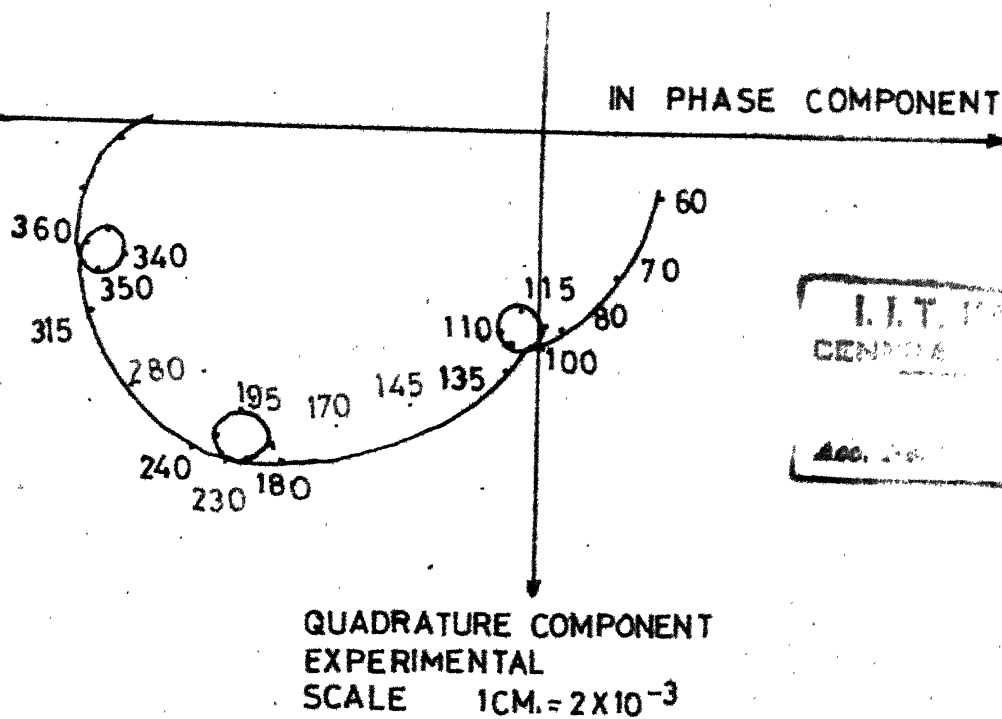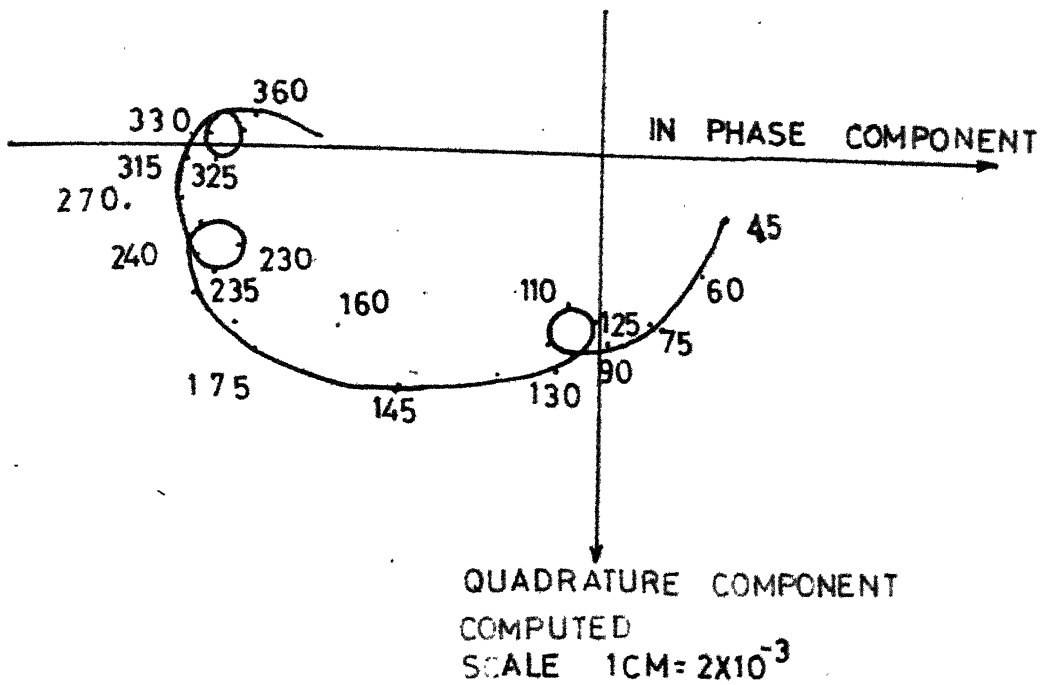
FREQUENCY IN C.P.S.

FIGURE # 11

IN PHASE COMPONENT

QUADRATURE COMPONENT
COMPUTED
SCALE   1CM = 2X10^{-3}

IN PHASE COMPONENT

QUADRATURE COMPONENT
EXPERIMENTAL
SCALE   1CM. = 2X10^{-3}

DIRECT   HARMONIC RESPONSE LOCUS
IN VERTICAL DIRECTION AT CENTRAL
RIB WITHOUT PORTAL

FIGURE # 12

DISPLACEMENT PLOT AT FOUNDATION

FREQUENCY C.P.S.
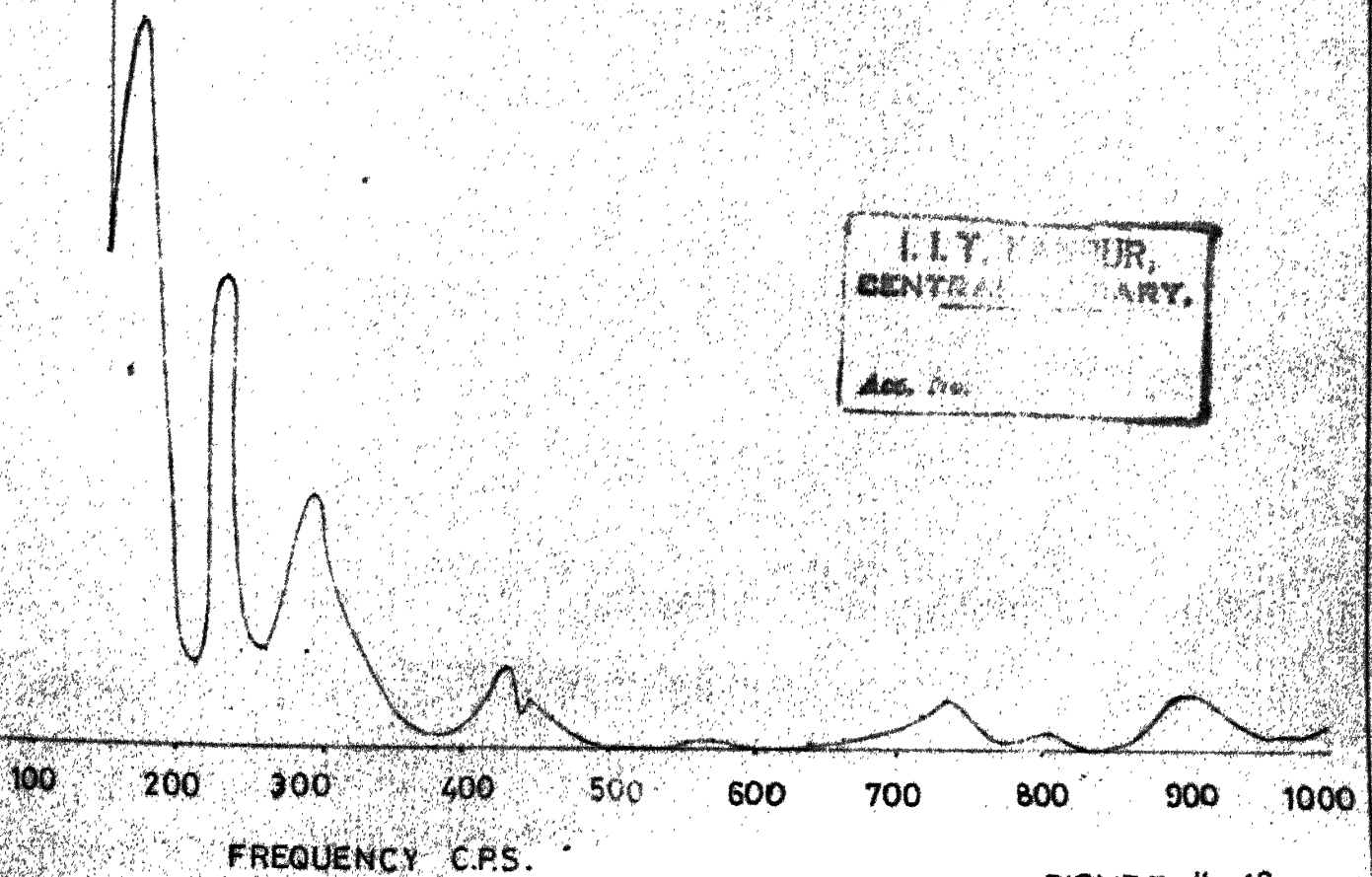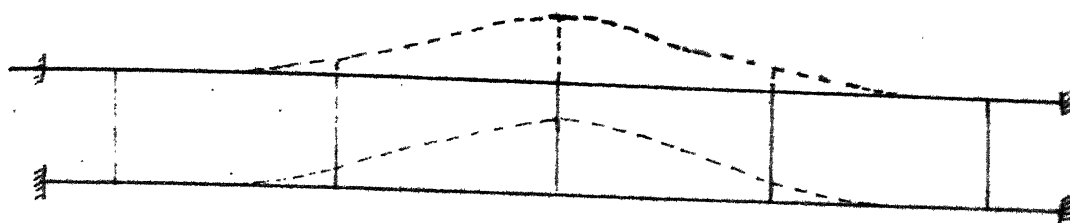
FIGURE # 13

FIRST MODE SHAPE
230 C.P.S.
VERTICAL DISPLACEMENTS
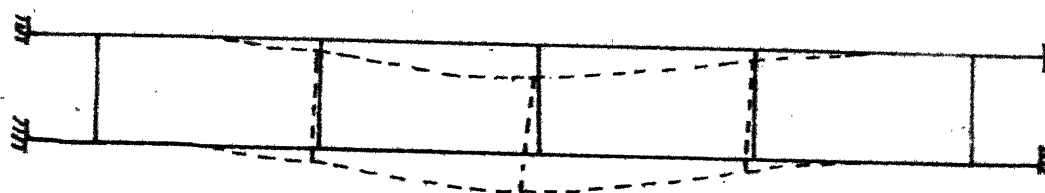
SECOND MODE SHAPE
260 C.P.S.
TRANSVERSE DISPLACEMENTS
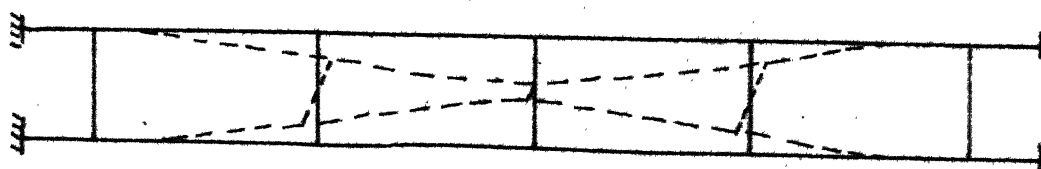
THIRD MODE SHAPE
440 C.P.S.
TORSIONAL DISPLACEMENTS

EXPERIMENTAL MODE SHAPES
WITHOUT PORTAL
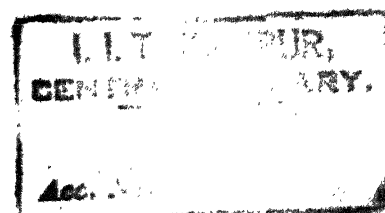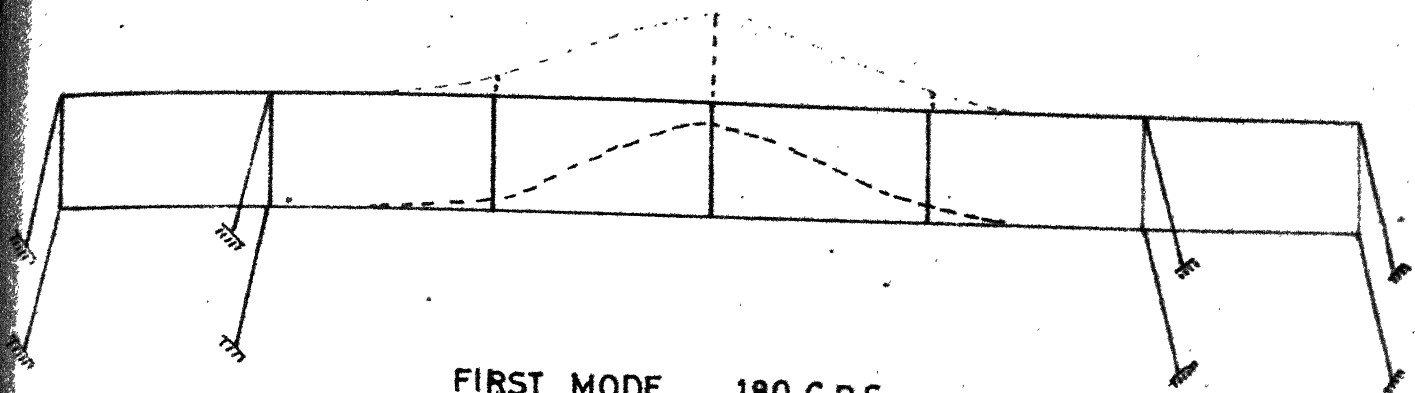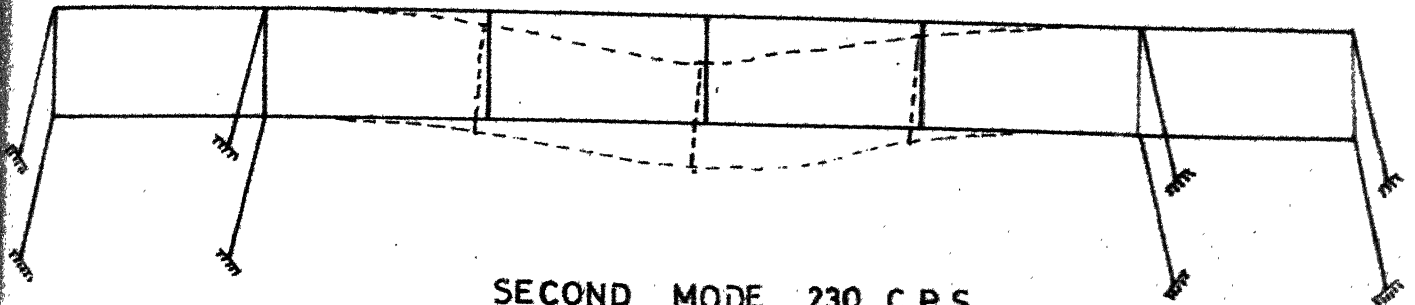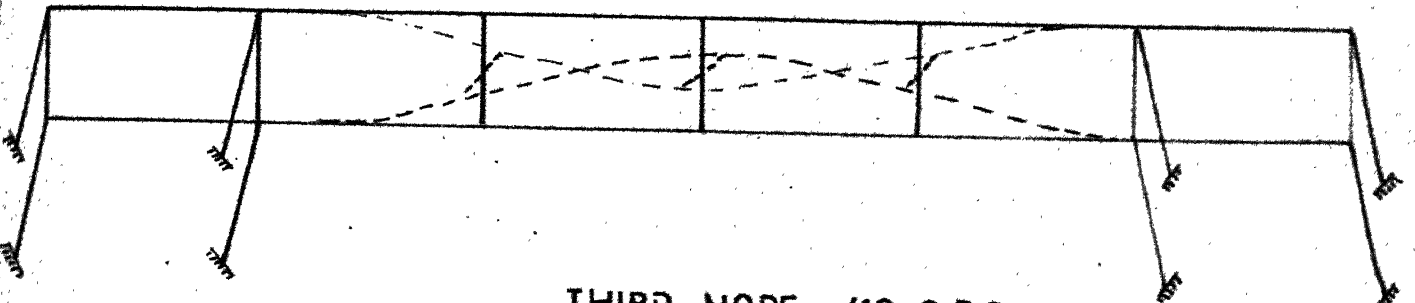
FIGURE #14·

FIRST MODE   180 C.P.S.
VERTICAL DISPLACEMENTS

SECOND MODE 230 C.P.S.
TRANSVERSE DISPLACEMENTS

THIRD MODE   410 C.P.S.
TORSIONAL DISPLACEMENTS

EXPERIMENTAL MODE SHAPES

WITH PORTAL

FIGURE # 15
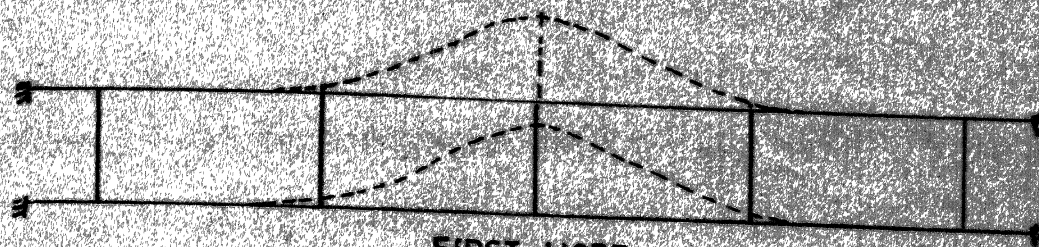
FIRST MODE 228 C.P.S.
VERTICAL DISPLACEMENTS
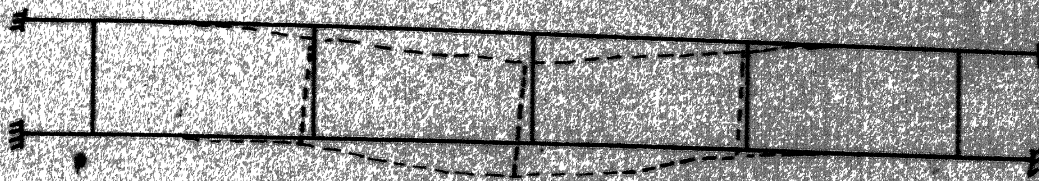
SECOND MODE 275 C.P.S.
TRANSVERSE DISPLACEMENTS
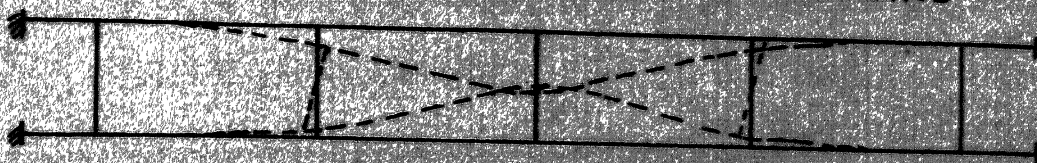
THIRD MODE 450 C.P.S.
TORSIONAL DISPLACEMENTS

COMPUTED MODE SHAPES
WITHOUT PORTAL

FIGURE # 16

FIRST MODE 200 C.P.S.
VERTICAL DISPLACEMENTS

SECOND MODE 240 C.P.S.
TRANSVERSE DISPLACEMENTS

THIRD MODE 425 C.P.S.
TORSIONAL DISPLACEMENTS
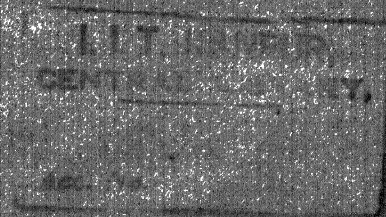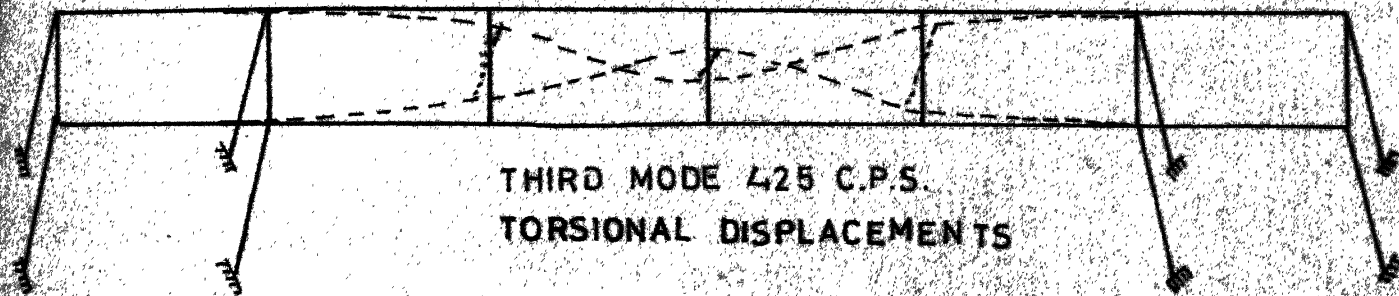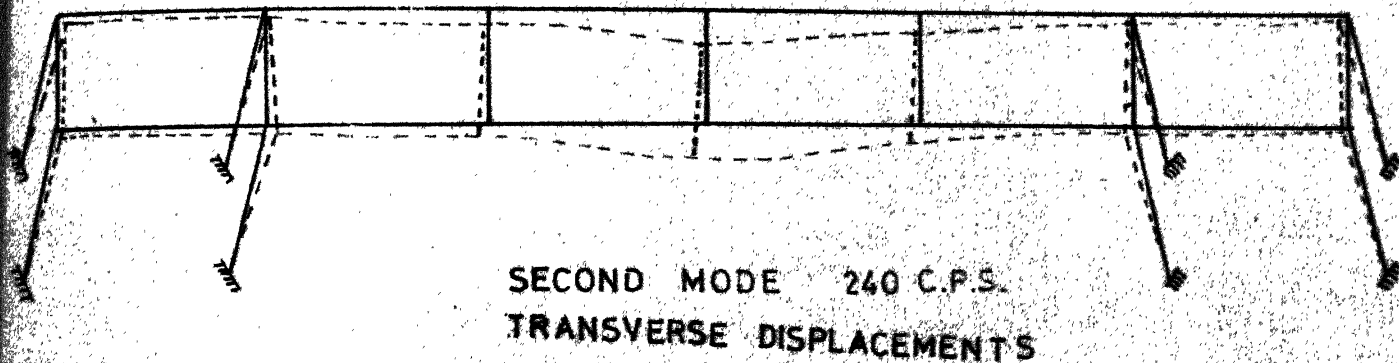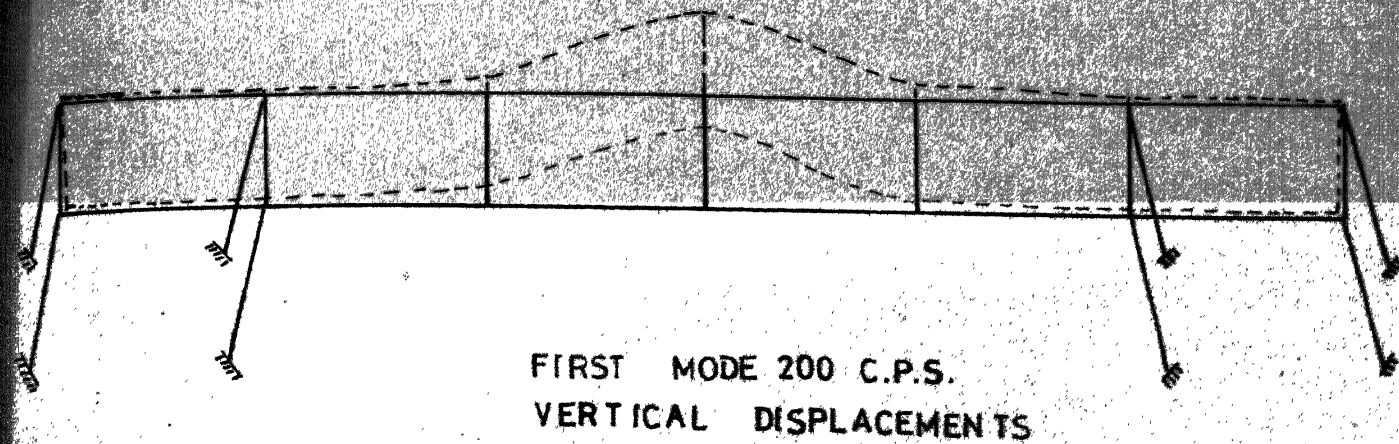
COMPUTED MODE SHAPES
WITH PORTAL
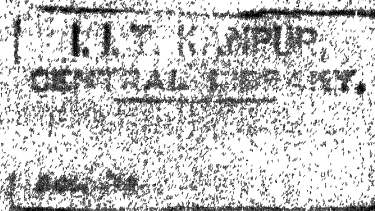
FIGURE # 17
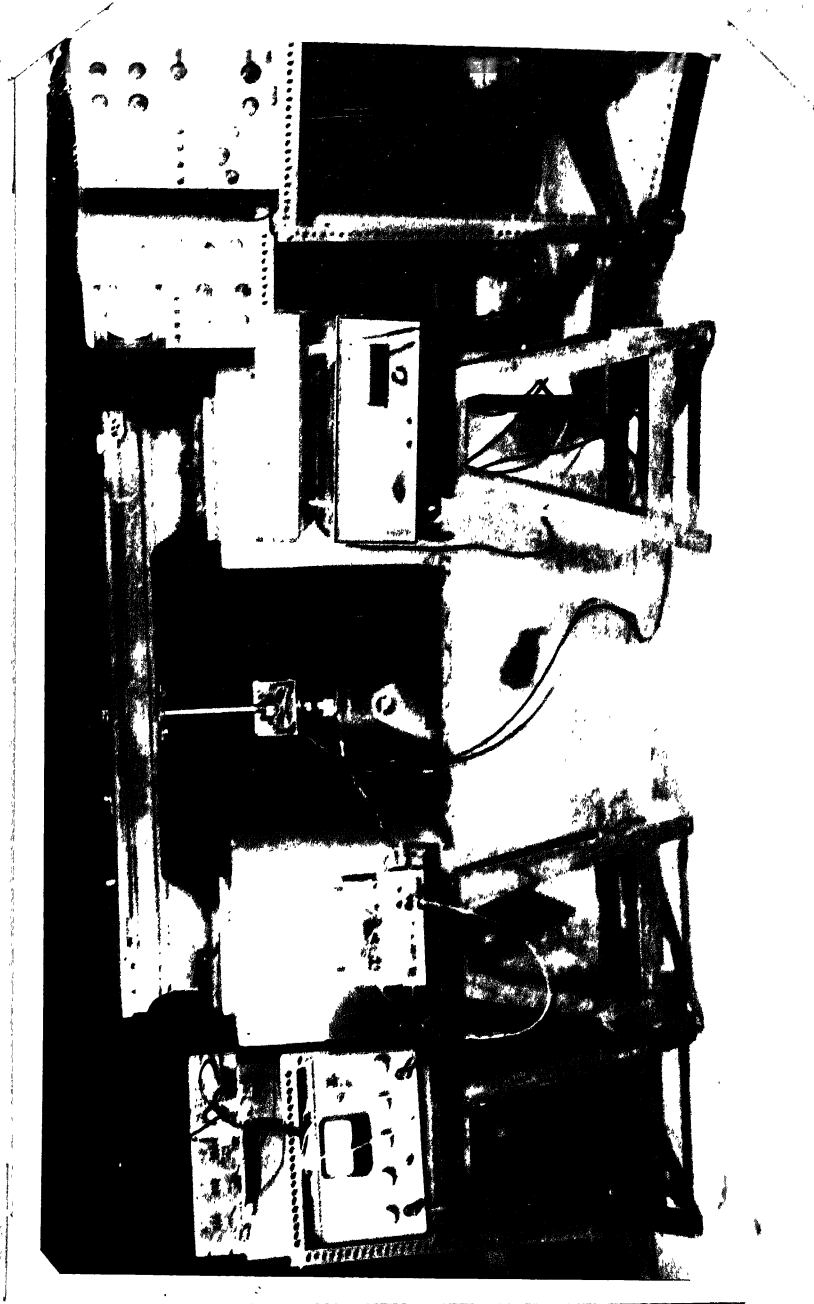
FIG.18   EXPERIMENTAL SET-UP WITH INSTRUMENTS
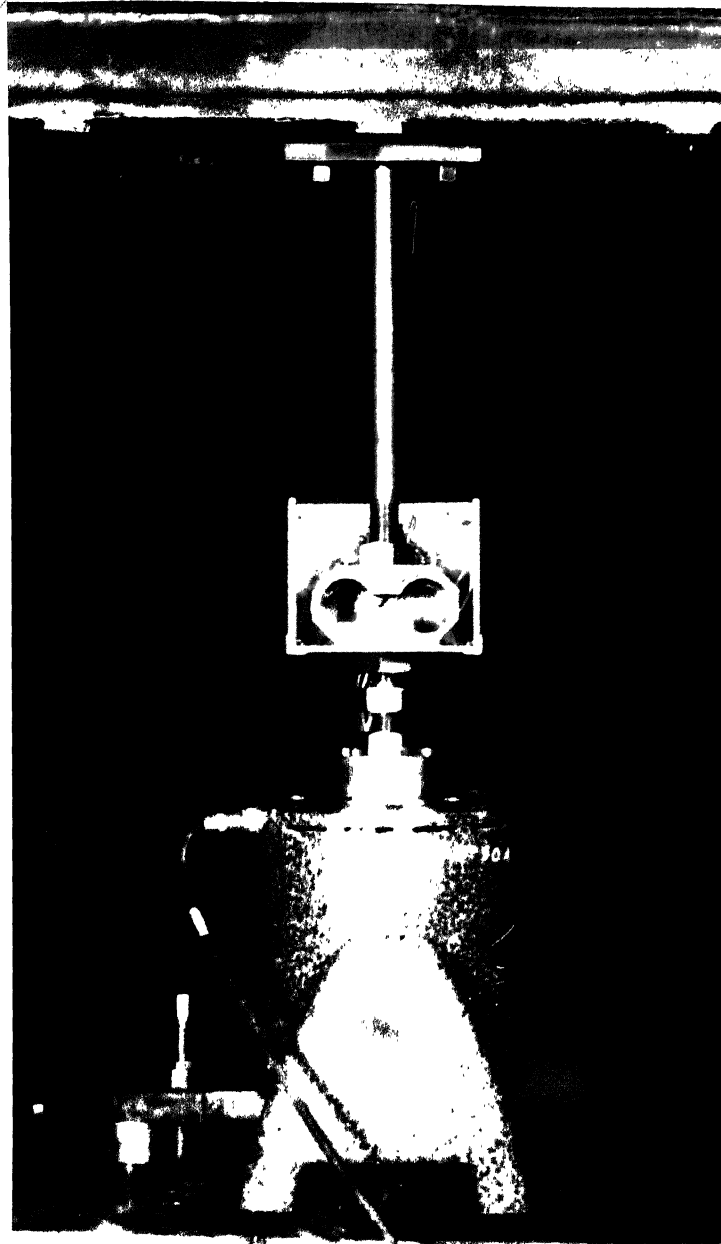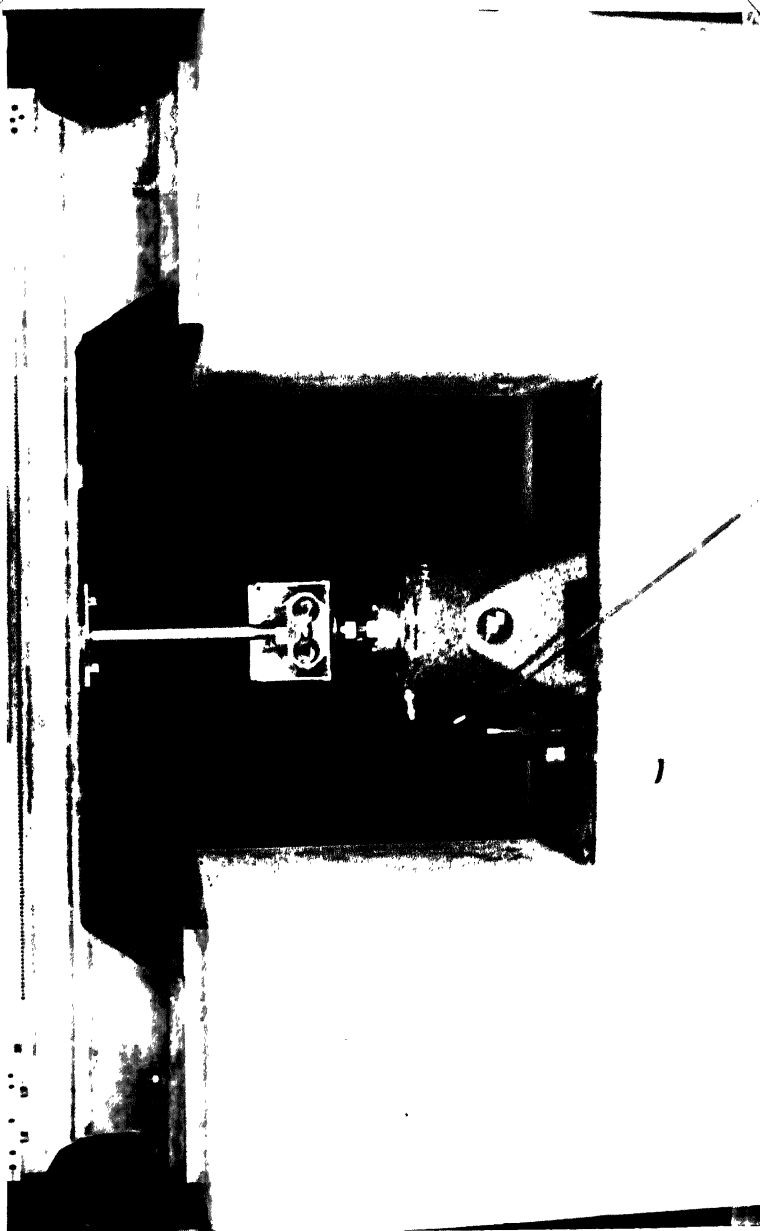
FIG .19   DYNAMOMETER CONNECTION WITH LATHE BED AND SHAKER
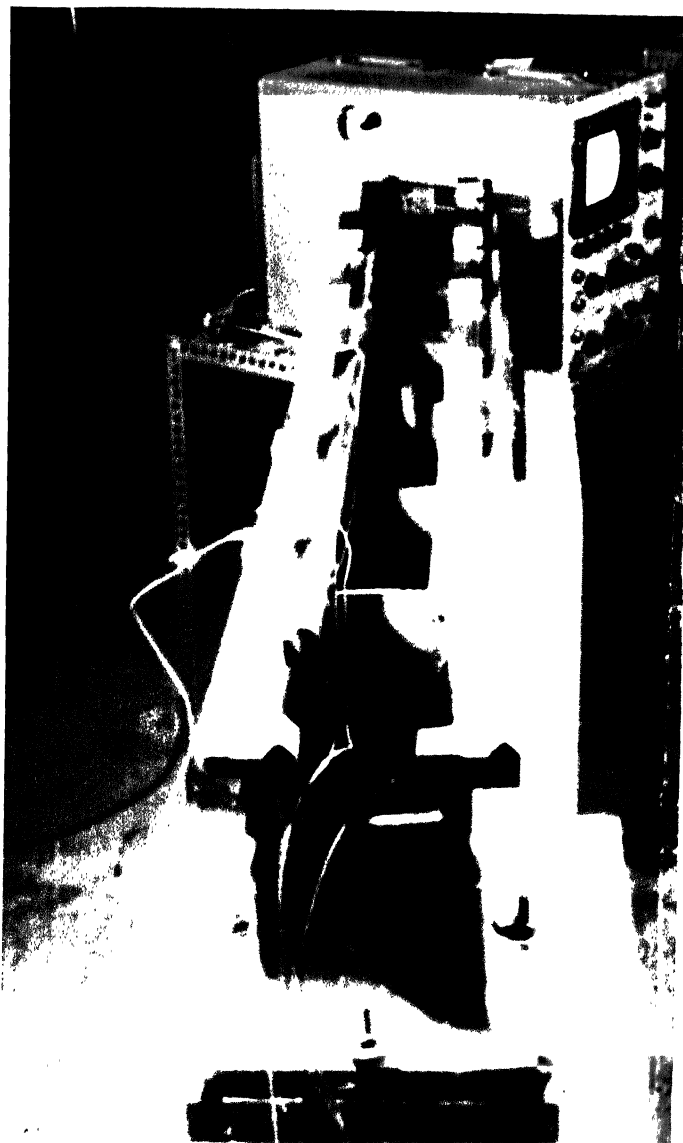
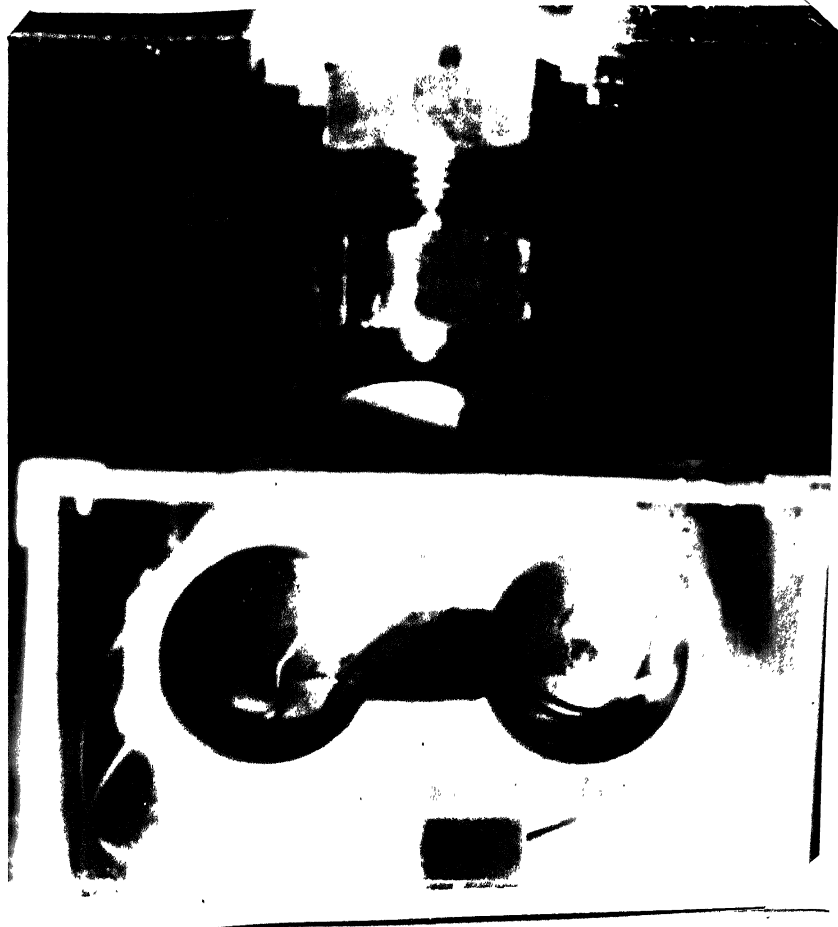FIG.20   COMPLETE LATHE BED ON FOUNDATION

FIG.21   POSITIONS OF ACCELEROMETERS ON THE LATHE BED

FIG.22   THE FORCE DYNAMOMETER